Lateral transduction is inherent to the life cycle of the archetypical *Salmonella* phage P22

Alfred Fillol-Salom[1,2,†], Rodrigo Bacigalupe[3,4,†], Suzanne Humphrey[1], Yin Ning Chiang[5], John Chen[5,*], José R Penadés[1,2,3,*].

[1]Institute of Infection, Immunity and Inflammation, College of Medical, Veterinary and Life Sciences, University of Glasgow, Glasgow, G12 8TA, UK.
[2]MRC Centre for Molecular Bacteriology and Infection, Imperial College London, SW7 2AZ, UK.
[3]Dep. Ciencias Biomédicas, Universidad CEU Cardenal Herrera, 46113, Moncada, Spain.
[4]The Rega Institute for Medical Research, KU Leuven, 3000, Leuven, Belgium.
[5]Department of Microbiology and Immunology, Infectious Diseases Translational Research Programme, Yong Loo Lin School of Medicine, National University of Singapore, 5 Science Drive 2, Singapore.

[†]These authors contributed equally.

Running title: Life cycle of temperate bacteriophages

Keywords: Lateral transduction, *Salmonella enterica*, pathogenicity islands, evolution, virulence, gene transfer, transduction, phage, P22.

[*]Corresponding authors: John Chen

Department of Microbiology and Immunology
Infectious Diseases Translational Research Programme
Yong Loo Lin School of Medicine
National University of Singapore
e-mail: miccjy@nus.edu.sg

José R. Penadés

Centre for Molecular Bacteriology and Infection
Imperial College London
e-mail: j.penades@imperial.ac.uk

Abstract

Lysogenic induction ends the stable association between a bacteriophage and its host, and the transition to the lytic cycle begins with early prophage excision followed by DNA replication and packaging (ERP). This temporal program is considered universal for P22-like temperate phages, though there is no direct evidence to support the timing and sequence of these events. Here we report that the long-standing ERP program is an observation of the experimentally favored *Salmonella* phage P22 tsc_2*29* heat-inducible mutant, and that wild-type P22 actually follows the replication-packaging-excision (RPE) program. We find that P22 tsc_2*29* excises early after induction, but P22 delays excision to just before it is detrimental to phage production. This allows P22 to engage in lateral transduction. Thus, at minimal expense to itself, P22 has tuned the timing of excision to balance propagation with lateral transduction, powering the evolution of its host through gene transfer in the interest of self-preservation.

Introduction

Bacteriophages (phages) are viruses that infect and replicate within bacteria. They are the most diverse and abundant biological entities on the planet, and they play an important role in controlling populations of bacteria that they exploit and kill. Yet their existence is tied to the success and survival of the hosts that they parasitize, and in the interest of self-preservation, phages can act as powerful agents of microbial adaptation and evolution by means of their ability to transfer bacterial DNA (encoding virulence factors and antibiotic resistance) from one bacterium to another by a process known as genetic transduction.

Phages are obligate intracellular parasites that follow two different life cycles. In the lysogenic cycle, although some are mantained as episomes, most temperate phages reproduce by integrating their genomes into the bacterial host chromosome where they persist in a dormant state as a prophage and replicate passively as part of the bacterial chromosome during cell division[1]. Infectious phage particles are produced in the lytic cycle, following host cell infection or prophage induction from the lysogenic cycle. In most of the archetypical studied viruses, including the *Salmonella enterica* P22 or the *Escherichia coli* λ phages, viral DNA replication first occurs bidirectionally, followed by a switch to rolling-circle replication that generates long DNA concatemers of multiple phage genomes[2,3]. The concatemeric DNA is packaged by the phage terminase enzyme (a hetero-oligomer of small and large terminase proteins), which recognizes a phage-specific packaging site (*pac* or *cos*) and cleaves the DNA to begin processing the genome into newly formed phage heads[4,5]. To complete DNA packaging, *pac*-type terminases make a nonspecific terminal cut when a capsid headful (slightly longer than a genome unit length) has been reached[6,7], while *cos*-type terminases require a second *cos* site to make the second cut[8], forming infectious phage particles that are released during bacterial cell lysis. It is also during this process that transducing particles are formed, when bacterial DNA is packaged into phage heads.

Lysogeny is generally very stable when maintained by sufficient levels of phage repressor, but prophages can switch to the lytic cycle when their hosts begin to deteriorate.

They usually do so by exploiting the bacterial SOS response, although additional mechanisms of prophage induction have been recently reported[9]. The SOS response is a global repair pathway that responds to DNA damage and serves as a proxy for the health of the host. Under normal conditions, the SOS-inducible genes are negatively regulated by the bacterial LexA repressor. After a cell experiences DNA damage, the bacterial RecA protein becomes activated by single-stranded DNA and acts as a co-protease to stimulate the self-cleavage of LexA[10,11]. This response is rapid and reversible, and complete LexA cleavage occurs in less than 5 minutes so that minor insults to the cell can be repaired in a timely manner[12]. Many phage repressors, such as those of phages λ and P22, mimic the structure of LexA and are also induce to undergo to self-cleavage by activated RecA[13]. However, phage repressors are cleaved far slower than LexA and take up to 30 minutes or longer to reach levels that are low enough to de-repress phage lytic genes[12,14,15]. Presumably, this is to ensure that lysogenic induction only occurs in cells that have received prolonged damaging exposure and are not expected to survive. Alternatively, the SOS response can be bypassed entirely with prophages that carry temperature-sensitive repressor (ts*c*) mutations. For instance, thermal induction of λ and P22 ts*c* mutants was the experimental method of choice for prophage de-repression because it occurred within minutes and the cultures were regarded as more synchronized[3,16].

After lysogenic induction, λ- and P22-like prophages are presumed to excise (and circularize) early as the first step in the temporal program of excision–replication–packaging (the ERP cycle; Fig. 1). This sequence of events is widely accepted and believed to be universal for these type of phages because it was thought that DNA packaging prior to excision would split the viral genome and prevent the production of infectious phage particles. Also, experimental support from λ and P22 studies showed that the proteins involved in excision (integrase and excisionase) were early gene products that appeared soon after phage infection or thermal induction of ts*c* mutants[3,16-18]. However, that appears to be the extent of the data on excision timing, and there seems to be no direct evidence that

validates the model for early excision[19]. Further complicating the matter, recently we found that some staphylococcal prophages delay excision until later in their lytic cycle[20], and others have shown that some *Salmonella* prophages likely do the same[21]. Therefore, the timing of prophage excision turns out to be an unresolved part of what was thought to be a well-defined phage life cycle. While the distinction between early or delayed prophage excision might seem minor, it has profound evolutionary consequences because only the latter is predicted to result in lateral transduction[20].

Phage-mediated gene transfer is known to occur by three different mechanisms: specialized (ST), generalized (GT), and lateral transduction (LT). In the first, specialized-transducing particles are formed when viral and bacterial DNA hybrid molecules are encapsidated following aberrant prophage excision events[22]. The mechanism is considered specialized because it is limited to the transfer of bacterial genes immediately adjacent to the integrated prophage. In the second, generalized-transducing particles are formed when *pac*-type terminases recognize *pac* site homologs in host DNA and initiate packaging by the headful mechanism[23]. The mechanism is regarded as generalized because any bacterial DNA can be packaged and transferred in this manner. In the recently discovered LT, transducing particles are formed when DNA packaging initiates from the bona fide *pac* sites of prophages that have delayed excision and are still attached to the bacterial chromosome[20,24]. The headful mechanism fills the first capsid with part of the prophage genome and continues through the adjacent bacterial chromosome for up to seven or more successive capsid headfuls. To prevent splitting the integrated viral genome in two, bidirectional *in situ* replication (prior to DNA packaging) creates sufficient genomic redundancy to enable LT and phage maturation to proceed in parallel. Together, this results in a mode of transduction that produces normal phage titers and transfers bacterial chromosomal DNA at frequencies far greater than previously observed for known mechanisms of host gene transfer. Importantly, LT was described using *S. aureus* phages,

raising the question whether this mechanism of gene transfer is exclusive to this species or widespread in nature.

Much of our current understanding of fundamental phage biology derives from the body of work on the archetypal *Salmonella pac*-type P22 and the *E. coli cos*-type λ phages. In those studies, λ or P22 ts*c* mutants were used for lysogenic induction because they were otherwise regarded as WT. Here we found that P22 follows two different temporal programs to produce infectious phage particles, depending on the method of lysogenic induction. Thermal induction of a P22 ts*c* mutant resulted in early prophage excision and the classical ERP program. SOS induction of P22 resulted in delayed prophage excision, DNA replication and packaging *in situ*, and LT (see scheme in Fig. 1). These results propose a new series of events in the life cycle of P22-like temperate prophages and show that early excision was an artifactual consequence of an experimental system and that delayed excision leading to LT are naturally parts of the phage life cycle.

Results

Lysogenic induction of the P22 or P22 tsc_2*29* prophages

As we noted earlier, prophage de-repression by thermal induction was known to occur much more rapidly than SOS induction[3,16]. This disparity in timing suggested that the heat-induced temporal program was either intact (but shifted ahead of schedule) or it was artificial. To distinguish these possibilities, we performed transcriptional profiling of P22 and P22 tsc_2*29*[25]. For phage infection, a non-lysogenic derivative of *Salmonella enterica* LT2 that was cured of all four of its resident prophages was infected with P22. For prophage induction, lysogenic strains were grown at permissive temperature (32°C) and for thermal induction the P22 tsc_2*29* lysogen was shifted to 42°C or to trigger the SOS response the P22 lysogen was treated with mitomycin C. Following thermal induction (for 30 minutes), the cultures were returned to 32°C because P22 (WT and tsc_2*29*) forms mostly particles that lack functional tails when incubated at high temperatures for prolonged periods[26]. Total RNA was harvested at 0, 30, 60, and 90 minutes after infection or induction for RNA-sequencing analysis. We

found that following SOS induction of the P22 prophage, most viral transcripts did not appear until 30 to 60 minutes and only reached maximal levels by 90 minutes, which was consistent with a gradation effect caused by the inactivation of the P22 repressor over time. In contrast, total viral transcripts reached maximal levels early (before 30 minutes) following infection, due to the total lack of repressor in naïve cells (Fig. 2). Surprisingly, thermal induction of P22 tsc_2*29* also resulted in maximal viral RNA levels before 30 minutes and mirrored the RNA transcript profiles of lytic infection, suggesting that the pool of P22 tsc_2*29* repressor was inactivated so completely and rapidly that the viral genome was de-regulated to the extent as it was during lytic infection. In fact, this prophage showed higher levels of *xis* and *int* expression even before induction (Fig. 2), suggesting that the c2 C59R mutant (present in P22 tsc_2*29*) is less capable of repressing transcription than WT, which ultimately affects prophage activation and the normal growth of the P22 tsc_2*29* lysogen. Therefore, compared to SOS induction of P22, the P22 tsc_2*29* program was shifted early, compacted to a small window of time, and no longer temporally regulated.

In the bottom strand, RNA transcripts of the integrase and excisionase genes (*int* and *xis*) appeared early (before 30 minutes) after P22 infection or thermal induction of P22 tsc_2*29*, but much later (between 30 and 60 minutes) after SOS induction of P22 (Fig. 2; Fig. S1). These results were consistent with the P22 tsc_2*29* literature and suggested that P22 tsc_2*29* excises much earlier than P22 following induction. To correlate the appearance of *int* and *xis* transcripts with prophage excision, the lysogenic strains were induced under the same conditions as above and total chromosomal DNA was isolated for whole-genome sequencing. Here we included ES18[27], a *Salmonella pac*-type phage with an unrelated DNA-packaging module, to broaden the scope of our study. For calculating the integration rates, we first counted the number of sequencing reads that spanned empty prophage attachment sites (*att*B), referred as chromosome-*att*B-chromosome reads; and the reads covering the left end of the integrated prophage (*att*L site), which represent reads covering the chromosome:*att*L region. At each time point, we compared the number of sequencing reads

covering the left end of the integrated prophage (*att*L) with the total number of reads mapping either the *att*B (empty) or the *att*L (integrated prophage) sites (see Fig. S2 for as schematic representation of the stategy used). The resulting value represents the percentage of integrated prophage

Prior to induction, spontaneous excision was observed for P22 tsc_2*29* (Fig. S2), owing to the general leakiness of transcription in the mutant (Fig. 2). Following lysogenic induction, the percentage of integrated P22 tsc_2*29* declined before 30 minutes, while those of P22 and ES18 remained steady before decreasing between 30 to 60 minutes (Fig. S2). These results were consistent with the transcriptomics data and confirmed that lysogenic induction by temperature shift or the SOS response results in early or delayed excision, respectively (Fig. S2). These differences in prophage induction were also evident when we anlaysed the production of the infective phage particles after induction of the different prophages (Fig. S3).

Thermal induction results in an artificial temporal program

Though the percentage of integrated P22 decreased from 30 to 60 minutes after SOS induction, it began to change course and increased after 60 minutes (Fig. S2). This curious result suggested that the P22 prophage was either reintegrating or replicating prior to excision. Previously, we had a similar observation with staphyloccocal prophages and found that *in situ* replication caused the late increase in the percentage of integrated prophage[20], so we constructed a deletion mutant of the P22 *pri* gene that initiates bidirectional (theta) replication and tested it for excision as above. Shown in Figure S2, the percentage of integrated P22 (Δ*pri*) now decreased from 60 to 90 minutes, confirming that P22 excision occurs late and that P22 replicates before excision.

To confirm that P22 replicates *in situ*, we checked for escape replication, which is a phenomenon that occurs when prophage replication starts before excision and amplifies the bacterial genome flanking the integrated prophage. For example, P22 prophage mutants that are “locked-in” (unable to excise) have been shown to initiate replication *in situ* and amplify neighbouring regions of the chromosome[28]. To test for this, we first deleted the *int* or *xis*

genes to generate P22 mutants that are unable to excise to serve as controls for escape replication. Then we infected the non-lysogenic strain with P22 or induced the lysogenic derivatives of P22 (WT, Δ*pri*, Δ*int*, and Δ*xis*) with mitomycin C or P22 tsc_2*29* with thermal induction and collected the total chromosomal DNA for whole-genome sequencing. At each time point, we quantified the reads corresponding to P22 and the host DNA adjacent to the *att*B_{P22} site and represented them as the coverage relative to the average of the entire genome. P22 infection showed early (before 30 minutes) and strong amplification of phage DNA (Fig. S4), which was consistent with the P22 literature[3,16-18]. SOS induction of the P22 lysogenic derivatives showed clear amplification of phage DNA later in the lytic cycle (Fig. 3), except for the P22 (Δ*pri*) mutant, which remained flat at all time points because it was unable to replicate.

P22 DNA amplification initiated between 30 to 60 minutes and was much more robust by 90 minutes when episomal replication occurred. By comparison, the P22 (Δ*int*) and P22 (Δ*xis*) mutants showed similar levels of phage DNA amplification at early times, but not at 90 minutes because they were not capable of episomal replication. Consistent with their inability to excise, amplification of the flanking bacterial DNA was higher for P22 (Δ*int*) and P22 (Δ*xis*) than P22 by 90 minutes (Fig. 3), although the phage titres of the *int* and *xis* mutant were significantly reduced (Fig. S3). These results confirm that P22 initiated replication while integrated and amplified the adjacent host DNA.

Compared to SOS induction of P22, thermal induction of the P22 tsc_2*29* mutant resulted in an altered replication pattern with much greater levels of phage DNA amplification at 0 and 30 minutes. It is likely that the higher levels of phage DNA amplification observed were due to early-onset episomal replication of the spontaneously-excised genomes (Fig. 3; Fig. 1), which also correlates to higher titres of the phages at the different time points analyzed (Fig. S3). Interestingly, the P22 tsc_2*29* mutant also amplified flanking bacterial DNA earlier (before 30 minutes) than P22 (Fig. 3), which was probably due to rapid de-repression of the entire P22 tsc_2*29* genome from thermal induction (Fig. 2).

236 To clearly confirm the previous results, we analysed excision and circularisation of the
237 different prophages after MC induction, using qPCR (Fig. S5). Taken together, all our results
238 show that thermal induction resulted in a program where the prophage genome separated
239 early from the bacterial chromosome before replication, while SOS induction resulted in
240 delayed prophage excision and an RPE program. Similar results were also observed for the
241 ES18 prophage (Fig. 3, Fig. S5), indicating that other *Salmonella* prophages initiate
242 replication *in situ* as well. Therefore, the heat-induced temporal program was not just early,
243 but it is artifactual as well.

244 **P22-mediated lateral transduction by SOS induction**

245 P22 is not known to engage in LT. Early studies that characterized theoretical modes of
246 phage transduction found that transductions with lysates from P22 tsc_2*29* lysogens (that
247 were heat-induced for longer than 75 minutes) did not support the models that most
248 resembled LT[29]. The main processes of LT are late prophage excision that link to DNA
249 replication and packaging *in situ*. Since thermal and SOS induction cause very different
250 temporal programs, we reasoned that they would result in equally different outcomes in
251 terms of *in situ* packaging and LT. To test for *in situ* DNA packaging, we inserted tetracycline
252 resistance markers (*tet*A) on both sides of the P22 *att*B site, in the directionality of phage
253 packaging (*tet*A^F) and in the opposite direction (*tet*A^R), to serve as proxies for bacterial gene
254 transfer. The locations of the markers were chosen in reference to the P22 *pac* site, which is
255 embedded in the center of the small terminase gene (*ter*S) and directs packaging
256 unidirectionally toward the 3' end[5,30]. The headful packaging mechanism reaches capacity
257 (~105% of the genome unit length) around 44kb, and the markers were placed so that there
258 would be sufficient flanking DNA for homologous recombination in the non-lysogenic
259 recipient. Additional markers in the directionality of terminase packaging were also
260 introduced at positions marking successive capsid headfuls to determine how much of the
261 bacterial chromosome could be mobilized from a single lysogen by the highly processive
262 DNA packaging machinery. These markers were also used for ES18 since both phages

integrate at the same *att*B site[27]. Non-lysogenic strains (deleted for the P22 *att*B site) carrying these markers were infected with P22, P22 tsc_2*29* and ES18 to assess GT or strains lysogenic for P22 tsc_2*29*, P22 and ES18 were induced to assess LT and the resulting lysates were tested as donors of tetracycline resistance to *S. enterica.*

We found that after SOS induction of the P22 lysogens, up to seven headfuls (>300 kb) were transferred at frequencies 2-3 orders of magnitude greater than by GT and remained greater than GT for up to twelve headfuls (>500 kb) (Fig. 4a). This P22-mediated LT occurred by the headful mechanism during lysogenic induction (Fig. S6), rather than by the superinfection of lysogenic strains by phages that were released early after SOS induction (Fig. S7). Importantly, similar results were also observed for ES18-mediated LT (Fig. 4b), suggesting that LT is widespread in *Salmonella* phages, as previously described in *S. aureus* phages[20]. While WT P22 and the P22 tsc_2*29* mutant showed similar efficiencies in mobilising markers by GT, the LT frequencies of the first two *tet*A^F markers were significantly lower after thermal induction of P22 tsc_2*29* than SOS induction of P22 (Fig. S8). This result likely explains why earlier studies did not observe LT with the P22 tsc_2*29* mutant. Taken together, these results show that P22 and ES18 engage in LT and transmit a large section of the *Salmonella* chromosome at high frequencies during SOS (but not thermal) induction. To expand our studies even further, we tested for LT in an *Enterococcus faecalis* lysogen of phage pp1[31]. As shown in Fig. S9, following SOS induction, prophage pp1 transferred *tet*M markers in the directionality of packaging at much higher frequencies than a marker in an unlinked location in the chromosome, showing that LT occurs in *E. faecalis* and it is a widespread and universal mechanism of gene transfer.

For a more direct visualization of LT, we purified P22 particles resulting from SOS induction and extracted the DNA for sequencing. The reads were quantified and mapped to the bacterial chromosome (NC_003197) and quantified based on coverage. We found that 96.5% of the reads of bacterial origin mapped to a 590 kb region in the directionality of packaging by P22-mediated LT. The remaining reads of bacterial origin were randomly

distributed along the whole genome, which was indicative of GT (Fig. 4c). The individual headfuls could be visualized by a step down in DNA packaging efficiency for each successive headful, corresponding to each re-initiation of DNA packaging by the processive terminase enzyme (Fig. 4d). Each step was approximately 44 kb in length, which matched the predicted headful capacity for P22.

The timing of prophage excision is tuned for lateral transduction in the newly identified P22 RPE cycle

Because early excision (by the P22 tsc_2*29* mutant) resulted in high phage titers (Fig. S3) and low levels of LT (Fig. S8), the opposite should be true for very late excision. This was indeed the case, as the P22 (Δ*int*) and P22 (Δ*xis*) single mutants or a P22 (Δ*int-xis*) double mutant resulted in much lower phage titers and higher levels of LT than WT P22 (Fig. S10). Matching results were obtained when different ES18 mutants were also analyzed (Fig. S10). Therefore, we wondered if there was a cost to P22 for delayed excision in terms of phage production. To test this, we designed a system in which prophage excision was tightly regulated and inducible. The P22 *int-xis* double mutant was complemented with a plasmid expressing the *int* and *xis* genes under the control of an arabinose-inducible promoter. To test for LT, we used the *tet*A^F marker located in the second P22 headful, thus avoiding any possible interference with ST. This strain was SOS-induced with mitomycin C [time (t) = 0 min] and arabinose was added at different time points ranging from 0 to 4h (after mitomycin C) for *int-xis* expression. As expected, early expression (t=0 mins) of the *int* and *xis* genes after SOS induction produced high phage titers but significantly reduced LT, while very late expression (t=240 mins) resulted in low phage titers and high levels of LT (Fig. 5). Interestingly, *int-xis* expression at 0 to 60 mins maintained P22 titers at the same high levels, with only a minor decline at 90 mins. At 120 to 240 mins, the phage titer declined rapidly, presumably because *in situ* DNA packaging compromised the integrity of the prophage genomes. By comparison, *int-xis* expression at 90 to 240 mins was optimal for LT. These results indicate that a delay in excision up to 60 to 90 minutes imposes a minimal cost to

317 phage production and allows P22 to engage in LT. Thus, P22 prophage excision occurs in a
318 narrow window of time that balances maximum phage production with LT.
319

Discussion

Phages have traditionally been viewed as selfish elements that exploit bacteria for their reproduction and spread in nature. The ERP program underscored this self-serving lifestyle because early prophage excision severed the connection to the bacterial cell and opened the way for unchecked viral propagation without any regard for the host. This sequence of events was based on the work from early studies with archetypal phages P22 and λ, and it has stood as the life cycle described for many temperate phages following lysogenic induction. However, phages are perhaps not as selfish as once presumed, and here we found that the temperate P22 phage life cycle is much more intimate and mutually beneficial than previously understood. Our results demonstrate, as ocurred with the *S. aureus* phages[20], that the P22 temperate phage does not follow the ERP program, but instead follow an RPE program, so that the prophage remains connected to the host chromosome for most of its life cycle following lysogenic induction. It does this by starting with *in situ* replication, which generates multiple copies of the integrated prophage to create genomic redundancy. Once the DNA packaging machinery is assembled, *in situ* packaging initiates from some of the integrated prophages and excision occurs from some of the others, so that the production of lateral-transducing particles occurs during normal phage maturation (see scheme in Fig. 1c).

Lysogenic protection and “morons” are the most common examples of benefits that temperate prophages provide to their bacterial hosts. In the first, prophages provide immunity against infection by other phages encoding identical or similar repressors. Phage morons are accessory genes that are not required for the phage life cycle but can increase the fitness of the lysogenic cell[32]. Importantly, defective prophages can still provide the benefits of lysogenic protection and morons, while prophages must be intact and functional to impart the benefits of LT. Thus, the RPE cycle (including LT) is an evolutionary force that preserves prophage integrity so that they remain intact and able to propagate. Moreover, we also propose here that LT is not just a universal mechanism of gene transfer, but an event that forms an intrinsic part of the life cycle of temperate *pac* prophages. We have recently

demonstrated that phages benefit from GT[33], and based on the frequency of gene transfer associated to this procces, we hypothesise that phages benefit even more from LT. Thus, once prophage genomes integrate into the bacterial chromosome, their fates are connected in a mutually beneficial relationship.

An interesting observation from our studies is that both *in situ* replication and *in situ* packaging must be perfectly coordinated to allow phages to engage in LT. This was best illustrated with P22 tsc_2*29*, where high levels of *in situ* replication were observed, but not high frequencies of LT, since most of the DNA packaging machinery was probably titrated away by the high levels of episomally replicating viral DNA. Likewise, our results also highlight the fine regulation that occurs between *in situ* packaging and late excision, which balances optimal phage reproduction with LT.

The RPE cycle may not just be an efficient evolutionary strategy that ensures efficient phage reproduction linked to high mobilization and transfer of the bacterial chromosome, but it could be also be an interesting mechanism used to overexpress some virulence genes under stress conditions. We have recently demonstrated that many pathogenicity islands are located next to *S. aureus* and *Salmonella* phage *att*B sites[20,34]. One can hypothesize that under stress conditions, the resident prophages in a subpopulation of cells will be induced. As a consequence of *in situ* replication, the copy number of virulence genes located next to *att*B sites will also increase, which can significantly augment the expression of particular host proteins. A handful of previous studies have shown that some *cos* phages, including the prototypical *E. coli* λ or the *S. enteritidis* Fels-1 that are not capable of engaging in GT or LT, replicate *in situ* before excision [21,35-37]. Although this idea is currently under study, these results suggest that the RPE cycle provides a fitness advantage to the phage and to the host beyond LT.

In summary, the results presented here re-write important concepts of P22 phage biology, including the series of events that occur after lysogenic induction. Moreover, these results also have potential to fundamentally re-structure our understanding of the roles

phages play in bacterial evolution, including the development of antimicrobial resistance and virulence in clinical strains.

Methods

Bacterial strains and growth conditions

Bacterial strains used in this study are listed on Table S2. *Salmonella enterica* strains were grown at 30°C, 37ºC or 42°C on Luria-Bertani (LB) agar or in LB broth with shaking (120 rpm). *Enterococcus faecalis* strains were grown at 37ºC on Brain Heart Infusion (BHI) agar or in BHI broth with shaking (120 rpm). For antibiotic selection, ampicillin (100 µg ml^{-1}), kanamycin (30 µg ml^{-1}), chloramphenicol (10 or 20 µg ml^{-1}) or tetracycline (3 or 20 µg ml^{-1}), from Sigma, was added when appropriate.

DNA methods

Gene insertions or deletions in *Salmonella* were performed as described[38]. Briefly, the chloramphenicol (*cat*), kanamycin (*km*R) or tetracycline (*tet*A) resistance makers were amplified by PCR, with primers listed in Table S3. PCR products were introduced by transformation into the appropriate recipient strains harbouring plasmid pKD46, which expresses the λ Red recombinase, and the markers were inserted in the bacterial or phage genome. The different mutants obtained were verified by PCR. To eliminate the marker, plasmid FLP helper pCP20 was transformed into the strains containing the resistance marker insertions. Strains containing the plasmid pCP20 were grown overnight at 30°C and a 1:50 dilution (with fresh LB) was prepared and grown for 4 h at 42°C to encourage plasmid loss and produce FLP recombination. Strains were plated out on LB plates and incubated for 24 h at 37°C. Individual colonies were streaked out and PCR was performed to corroborate that the chromosomal marker had been removed and were sequenced by Sanger sequencing (Eurofins Genomics).

Insertion of a *tet*M cassette into the *E. faecalis* chromosome was performed by double recombination using allelic exchange plasmid pBT2bgal. Briefly, plasmids pJP2563,

pJP2564, pJP2565, pJP2566 and pJP2568 were introduced into *E. faecalis* V583-derivative strains VE18990 (pp-) and VE18562 (fp1) by transformation, with selection at 32°C on BHI agar supplemented with 10 μg ml^{-1} chloramphenicol. Following two rounds of sequential incubation at 32°C and 42°C, as previously described[39], individual tetracycline-resistant, chloramphenicol-sensitive colonies were selected, and PCR was performed to confirm the correct placement of the tetracycline marker in the bacterial chromosome. Sanger sequencing (Eurofins Genomics) of PCR products corroborated marker placement.

Plasmid construction

Plasmid pJP2534 (Table S4) was generated by cloning the PCR product containing the P22 *int-xis* region, amplified with the oligonucleotides listed in Table S3 (Sigma), into the pBAD18 vector. The cloned plasmid was verified by Sanger sequencing (Eurofins Genomics).

For insertion of *tetM* into the *E. faecalis* chromosome, we made use of the thermosensitive allelic exchange plasmid pBT2bgal. Briefly, the *E. faecalis* chromosomal regions flanking the proposed *tetM* insertion site were amplified by PCR using the oligonucleotides listed in Table S3. The *tetM* cassette was amplified from plasmid pRN6680[40] using the oligonucleotides indicated. Overlap extension PCR was used to produce chromosomal left flank-*tetM* fusion products, which were cloned into pBT2bgal alongside the right-flank PCR product, generating plasmids pJP2563, pJP2564, pJP2565, pJP2566 and pJP2568 (Table S4). All plasmid sequences were verified by Sanger sequencing (Eurofins Genomics).

Induction experiments

For *Salmonella* phage induction, overnight cultures of lysogenic donor strains were diluted 1:50 in fresh LB broth, then grown at 32°C and 120 rpm until an OD_{600} of 0.2 was reached. Prophages were induced by either addition of mitomycin C (MC) (2 μg ml^{-1}) or by shifting the temperature to 42°C (30 minutes) for thermal induction. Following induction, cultures were incubated at 32°C with slow shaking (80 rpm). Cell lysis occurred 3-4 h post-induction.

For *E. faecalis* phage induction, overnight cultures of lysogenic donor strains were diluted 1:25 into fresh BHI broth, then grown at 37^{o}C, 120 rpm until an OD_{540} of 0.10 was reached. Prophages were induced by addition of MC (2 µg ml^{-1}). Following induction, cultures were incubated at 32^{o}C, 80 rpm for 5.5 h to permit cell lysis. Cell lysis occurred 4-5 h post-induction.

Infection experiments

For *Salmonella* phage infection, recipient strains were diluted 1:50 in fresh LB broth and incubated at 32°C and 120 rpm until an OD_{650} of 0.15 was reached. The culture was then centrifuged for 5 min at 4 °C/3,000 x *g*. The supernatant was discarded, and the pellet re-suspended at a ratio 1:1 of LB-phage buffer (phage buffer [PHB]: 1 mM NaCl, 0.05M Tris pH 7.8, 1 mM $MgSO_4$, 4 mM $CaCl_2$). The culture was then infected with a phage lysate at a ratio of 1:1 and incubated at 32°C with slow shaking (80 rpm). Generally, cell lysis occurred 4-5 h post-infection.

For *E. faecalis* phage infection, recipient strains were diluted 1:25 into fresh BHI broth, then grown at 37^{o}C, 120 rpm until an OD_{540} of 0.34 was reached. 55 µl of recipient cells were mixed with 100 µl phage lysate diluted in PHB (2.0 x10^{7} Φp1 PFU, yielding an infection ratio of 1:1), and incubated at room temperature for 10 mins before addition of 3 ml phage top agar (PTA: 20 g Nutrient broth no. 2, 3.5 g agar, 10 mM $MgCl_2$). The entire volume was poured onto phage base agar (PBA: 25 g of Nutrient Broth No. 2, Oxoid; 7g agar, Formedium) supplemented with 10mM $MgCl_2$, then incubated at 37^{o}C for 16-18 h. Phage plaques were harvested by collecting and resuspending the PTA layer in 3 ml PHB. Samples were vortexed for 20s, then centrifuged for 10 minutes at 4000 x *g*, and the resulting supernatants were filter sterilized.

Phage lysates obtained either by infection or induction were filtered using sterile 0.2 µm filters (Minisart® single use syringe filter unit, hydrophilic and non-pryogenic, Sartonium Stedim Biotech) and the number of phage or transducing particles quantified.

452 **Phage titration and transduction**

453 For *Salmonella* phage titres, serial dilutions of phage lysates were prepared in PHB, and 100
454 µl of diluted lysate was used to infect 50 µL of cells at OD_{600} 0.34 for 10 min at room
455 temperature. For *E. faecalis* phage titres, serial dilutions of phage lysates were prepared in
456 PHB, and 100 µl of diluted lysate was used to infect 55 µL of VE18590 (pp-) recipient cells at
457 OD_{540} 0.34 for 10 min at room temperature. Following incubation, 3 ml PTA (supplemented to
458 a final concentration of 10 mM with $CaCl_2$, for *Salmonella* phages, or $MgCl_2$, for *E. faecalis*
459 phages) was added to stop the infection process, and the different combinations of
460 culture:phage dilutions were plated out on PBA supplemented to a final concentration of 10
461 mM with either $CaCl_2$ or $MgCl_2$ as appropriate. PBA plates were incubated at 37°C for 24h
462 and the number of plaques quantified as plaque forming units (PFU)/ml.

463 For transductions, a total of 1ml of *Salmonella* recipient cells at OD_{600} of 1.4
464 supplemented with 4.4mM of $CaCl_2$ or 1ml of *E. faecalis* recipient cells at OD_{540} of 1.4
465 supplemented with 4.4mM of $MgCl_2$, were infected for 30 mins at 37°C with the addition of
466 100 µL of phage lysate diluted in PHB. Following incubation, 3 ml LB top-agar (LTA: 20g LB,
467 Sigma; 7.5 g agar, Formedium) or BHI top-agar (BTA: 37g BHI, Oxoid; 7.5g agar,
468 Formedium) was added to stop the transduction process, and the entire contents were
469 poured onto LBA (*Salmonella*) or BHI (*E. faecalis*) agar plates containing the appropriate
470 antibiotic. Plates were incubated at 37°C for 24h (*Salmonella*) or 36h (*E. faecalis*) and the
471 number of colonies formed (transduction particles present in the lysate) were counted and
472 represented as the transduction forming units (TFU)/ml. Results were generally reported as
473 the transduction units (TrU/10^9 PFU), which represents the number of transducing particles
474 per 1E+9 of PFU.

475 **Co-transduction analyses**

476 The frequency of marker co-transduction was determined using lysates generated either by
477 phage induction or by phage infection of the strains containing both resistance markers (*cat*

478 and *tet*A), at varying distances apart. 100 *tet*A-resistant transductants were tested for *cat*
479 resistance and the results were represented as the frequency of (*cat*/*tet*A) x 100%.
480

Inducible complementation of the P22 Δ*int-xis* mutant

The P22 Δ*int-xis* lysogens complemented in trans with the pBAD18 derivative plasmid expressing the *int-xis* genes were diluted 1:50 (in fresh LB broth supplemented with ampicillin at 100 μg ml^{-1}) and were grown at 32°C, 120 rpm until an OD_{600} of 0.2 was reached. Cultures were induced with MC (t=0) and incubated at 32°C with slow shaking (80 rpm). Arabinose (0.02%) was added at 0, 30, 60, 90, 120, 150, 180 and 240 min post-induction for complementation of *int-xis* functions. Cultures were filtered using sterile 0.2 μm filters and the number of phage and transducing particles in the resultant lysate were quantified.

Whole genome sequencing (*in situ* replication)

Samples were induced as described in previous sections. At the indicated time points after MC-induction, 12 ml of sample was collected and DNA extraction was performed using the 'ChargeSwitch® gDNA Mini Bacteria Kit' from Thermo Fisher Scientific, following the manufacturer's instructions. The DNA was precipitated by 0.3M NaOAc and 2.25 volume of 100% ethanol, then pelleted at 12,000 x g for 30 min at 4ºC and washed once with 1 ml of 70% ethanol. After centrifugation, the DNA pellets were air dried for 30 min and resuspended in 50 μl nuclease free water. Quality control of DNA samples was tested using Agilent Bioanalyzer 2100 and whole genome sequencing (WGS) was performed at the University of Glasgow Polyomics Facility using Illumina TruSeq DNA Nano library prep, obtaining 2x75 bp pair end reads with DNA PCR free libraries. A total of 2.2M reads were generated and trimmed reads were mapped to the appropriate genome: P22 (NC_002371.2), ES18 (NC_006949) and LT2 (NC_003197). Only one replicate was sequenced per experiment.

Whole genome sequencing (phage DNA from capsid extraction)

A total of 100 ml P22 phage lysate was produced by MC induction. Phage lysates were treated with RNase (1 μg ml^{-1}) and DNase (10 μg ml^{-1}) for 30 min at room temperature. Followed by addition of 1 M of NaCl to the lysate for 1 h on ice. After incubation, the mix was

centrifuged at 11,000 x *g* for 10 min at 4°C, and phages were resuspended with 10% wt/vol polyethylene glycol (PEG) 8000 and kept overnight at 4ºC. Phages were precipitated at 11,000 x *g* for 10 min at 4°C and resuspended in 1 ml of phage buffer. The precipitated phages were loaded on the CsCl step gradients (1.35, 1.5 and 1.7 g ml^{-1} fractions) and centrifuged at 80,000 x *g* for 2h at 4°C. The phage band was extracted from the CsCl gradients using a 23-gauge needle and syringe. Phages were dialyzed overnight to remove CsCl excess using SnakeSkin™ Dialysis Tubing (3.5K MWCO, 16mm dry) into 50mM of Tris pH 8 and 150mM NaCl buffer.

Following CsCl purification, phage lysates were treated with DNase (10 µg ml^{-1}) for 30 min at room temperature and DNase was inactivated with 5mM EDTA for 10 min at 70°C. Phage lysate was combined with an equal volume of lysis mix (2% SDS and 90 µg ml^{-1} proteinaseK) and incubated at 55ºC for 1 h. DNA was extracted with an equal volume of phenol:chloroform:isoamyl alcohol 25:24:1 and samples were centrifuged at 12,000 x *g* for 5 min, and the aqueous phase containing the DNA was obtained. DNA was ethanol precipitated as already described, and the resulting DNA was resuspended in 100 µl nuclease free water.

Quality control of DNA samples was tested using Agilent Bioanalyzer 2100 and WGS was performed at the University of Glasgow Polyomics Facility using Illumina TruSeq DNA Nano library prep, obtaining 2x75 bp pair end reads with DNA PCR free libraries. A total of 3000X bacterial genome coverage, 104M reads, were generated and trimmed reads were mapped to the appropriate genome: P22 (NC_002371.2) and LT2 (NC_003197). Only one replicate was sequenced per experiment.

WGS analysis

We first used FastQC v0.11.8 (http://www.bioinformatics.babraham.ac.uk/projects/fastqc/) to assess the quality of the sequencing reads and Trimmomatic v0.3 to remove adapters and low-quality reads. Sequencing reads from each experiment were mapped to their respective reference genomes using the Burrows-Wheeler Alignment Tool 0.7.17

(https://academic.oup.com/bioinformatics/article/25/14/1754/225615). Picard-tools v2.1.1 (http://broadinstitute.github.io/picard/; Broad Institute) was next used to obtain the bam files, which were merged with SAMtools v1.11[41], sorted and indexed; and Bedtools *bamtobed* v2.30.0[42] was used to produce the bed files. We computed the relative coverage over 100 sliding windows along the entire chromosome for each of the experiments. For this, we computed the average coverages across the full genome without phages, which were removed using bedtools subcommand *subtract*. Subsequently, the coverages across the sliding windows were divided by the chromosomal averages. In order to estimate the percentage of integration, we calculated the number of reads that spanned the bacterial chromosome and phages on the two ends of the P22 and ES18 phages. In addition, we counted the sequencing reads spanning the empty prophage attachment sites (*att*B) and the reads covering the left end of the integrated prophage (*att*L site). This was performed using the *'view'* subcommand of samtools and filtering by the coordinates of the mapping reads and their respective lengths. Next, the integration percentages were obtained by dividing the reads covering the chromosome-*att*L-prophage (chr:pha) by the total reads (chr:pha + chr:chr). Fisher tests on the sequencing read counts (chromosome-*att*B-chromosome reads and chromosome-*att*L-prophage reads) between different time points (0 min vs 30 min, 30 min vs 60 min, and 60 min vs 90min) indicate that all apparent changes are statistically significant.

Finally, the sequencing reads of the capsids were rarefied by subsampling 100 million reads from each of the paired, filtered reads using seqtk v1.3 *sample* command (Toolkit for processing sequences in FASTA/Q formats. Available from: https://github.com/lh3/seqtk.). Reads were mapped to the NC_003197 reference genomes and processed as above. The absolute coverage was calculated using bedtools by 100 bp windows across the entire genome. Assemblies of the content of the capsids were obtained using SPAdes v3.12[43].

Total RNA extraction and mRNA enrichment

Following induction of lysogenic strains, 30 ml samples were collected at the indicated time points post-MC addition, and cell pellets were harvested by centrifugation at 5,000 x *g* for 5 min. The bacterial pellet was resuspended in TE buffer (10 mM Tris-Cl, 1 mM EDTA, pH 8.0) containing lysozyme (50 mg ml^{-1}) and was lysed in a FastPrep-24 homogenizer (MP Biomedicals) using two cycles of 60 s at 6.5 m s-2 interrupted by a 5 minutes incubation on ice. Total RNA was extracted using a RNeasy kit (Qiagen) according to the manufacturer's instructions and genomic DNA was removed using TURBO DNase (Ambion, Carlsbad, CA, USA). RNA samples were enriched for mRNA using MICROBexpress mRNA enrichment kit (Ambion). Quality control of RNA-seq samples for mRNA enrichment was tested using Agilent Bioanalyzer 2100 at the University of Glasgow Polyomics Facility. Experiments were performed in triplicate.

RNA-seq transcriptome analysis

cDNA synthesis and sequencing, 75 bp single end reads, was performed at the University of Glasgow Polyomics Facility using Illumina NextSeq 500. The sequencing reads were processed using Trimmomatic v0.3[44] for removal of adapters and low quality reads. Transcriptomic analyses were performed using the pipeline READemption v0.4.3[45]. First, we created individual projects for each experiment using the create subcommand and the fasta and annotation files of the reference genome (P22: NC_002371) were transferred to the corresponding locations. Next, we performed the alignment step using default parameters, and the coverage was computed using only the uniquely aligned reads, normalizing by these reads. The strand specific coverage counts normalized by 100,000 division were used for the final analyses. Strands coverage values of the phage spanning regions for different replicates were plotted with values >1 log10 corrected.

Quantitative PCR (qPCR)

Samples were temperature or MC-induced and at the indicated time points, and 6 ml of each sample was collected for DNA extraction, as previously indicated. qPCR was performed using the Power Up SYBR Green master mix on the Applied Biosystems StepOnePlus

system. Two nanogram of DNA was used per reaction with primers listed in Table S3 at 10 µM final concentration. *rap*A was used as a reference gene.

The relative excision or circularisatiopn levels within distinct experiments were determined with the $2^{-\Delta CT}$ method[46].

Statistical analyses

All statistical analyses were performed as indicated in the figure legends using GraphPad Prism 6.01 software. Statistical value for each experiment is listed in Table S1.

Data availability

Source data are provided with this paper. The WGS and RNAseq data generated in this study have been deposited in the NCBI SRA database under accession code BioProject PRJNA737196 [https://www.ncbi.nlm.nih.gov/bioproject/737196].

The different accession numbers (obtained from the NCBI database) for reference genomes and the bioinformatics analyses are: LT2 (NC_003197), P22 (NC_002371.2) and ES18 (NC_006949).

References

1. Howard-Varona, C., Hargreaves, K. R., Abedon, S. T. & Sullivan, M. B. Lysogeny in nature: mechanisms, impact and ecology of temperate phages. *ISME J* **11,** 1511–1520 (2017).
2. Court, D. L., Oppenheim, A. B. & Adhya, S. L. A new look at bacteriophage lambda genetic networks. *J. Bacteriol.* **189,** 298–304 (2007).
3. Susskind, M. M. & Botstein, D. Molecular genetics of bacteriophage P22. *Microbiol. Rev.* **42,** 385–413 (1978).
4. Casjens, S. R. The DNA-packaging nanomotor of tailed bacteriophages. *Nat. Rev. Microbiol.* **9,** 647–657 (2011).
5. Rao, V. B. & Feiss, M. The bacteriophage DNA packaging motor. *Annu. Rev. Genet.* **42,** 647–681 (2008).
6. Streisinger, G., Edgar, R. S. & Denhardt, G. H. Chromosome structure in phage T4. I. Circularity of the linkage map. *Proc. Natl. Acad. Sci. U.S.A.* **51,** 775–779 (1964).
7. Streisinger, G., Emrich, J. & Stahl, M. M. Chromosome structure in phage T4, iii. Terminal redundancy and length determination. *Proc. Natl. Acad. Sci. U.S.A.* **57,** 292–295 (1967).
8. Feiss, M. & Siegele, D. A. Packaging of the bacteriophage lambda chromosome: dependence of *cos* cleavage on chromosome length. *Virology* **92,** 190–200 (1979).
9. Silpe, J. E. & Bassler, B. L. A Host-produced quorum-sensing autoinducer controls a phage lysis-lysogeny decision. *Cell* **176,** 268–280.e13 (2019).
10. Little, J. W. & Mount, D. W. The SOS regulatory system of *Escherichia coli*. *Cell* **29,** 11–22 (1982).
11. Little, J. W. The SOS regulatory system: control of its state by the level of RecA protease. *J. Mol. Biol.* **167,** 791–808 (1983).
12. Little, J. W. LexA cleavage and other self-processing reactions. *J. Bacteriol.* **175,** 4943–4950 (1993).
13. Sauer, R. T., Ross, M. J. & Ptashne, M. Cleavage of the lambda and P22 repressors by RecA protein. *J. Biol. Chem.* **257,** 4458–4462 (1982).
14. Little, J. W. Autodigestion of LexA and phage lambda repressors. *Proc. Natl. Acad. Sci. U.S.A.* **81,** 1375–1379 (1984).
15. Phizicky, E. M. & Roberts, J. W. Kinetics of RecA protein-directed inactivation of repressors of phage lambda and phage P22. *J. Mol. Biol.* **139,** 319–328 (1980).
16. Liu, X., Jiang, H., Gu, Z. & Roberts, J. W. High-resolution view of bacteriophage lambda gene expression by ribosome profiling. *Proc. Natl. Acad. Sci. U.S.A.* **110,** 11928–11933 (2013).
17. Casjens, S. R. & Hendrix, R. W. Bacteriophage lambda: Early pioneer and still relevant. *Virology* **479-480,** 310–330 (2015).
18. Lew, K. & Casjens, S. Identification of early proteins coded by bacteriophage P22. *Virology* **68,** 525–533 (1975).
19. Davidson, A. R. A common trick for transferring bacterial DNA. *Science* **362,** 152–153 (2018).
20. Chen, J. *et al.* Genome hypermobility by lateral transduction. *Science* **362,** 207–212 (2018).

21. Frye, J. G., Porwollik, S., Blackmer, F., Cheng, P. & McClelland, M. Host gene expression changes and DNA amplification during temperate phage induction. *J. Bacteriol.* **187,** 1485–1492 (2005).

22. Morse, M. L., Lederberg, E. M. & Lederberg, J. Transduction in *Escherichia coli* K-12. *Genetics* **41,** 142–156 (1956).

23. Zinder, N. D. & Lederberg, J. Genetic exchange in *Salmonella*. *J. Bacteriol.* **64,** 679–699 (1952).

24. Chiang, Y. N., Penadés, J. R. & Chen, J. Genetic transduction by phages and chromosomal islands: The new and noncanonical. *PLoS Pathog.* **15,** e1007878 (2019).

25. Levine, M. & Smith, H. O. Sequential gene action in the establishment of lysogeny. *Science* **146,** 1581–1582 (1964).

26. Israel, V. The production of inactive phage P22 particles following induction. *Virology* **33,** 317–322 (1967).

27. Casjens, S. R. *et al.* The generalized transducing *Salmonella* bacteriophage ES18: complete genome sequence and DNA packaging strategy. *J. Bacteriol.* **187,** 1091–1104 (2005).

28. Youderian, P., Sugiono, P., Brewer, K. L., Higgins, N. P. & Elliott, T. Packaging specific segments of the *Salmonella* chromosome with locked-in Mud-P22 prophages. *Genetics* **118,** 581–592 (1988).

29. Kwoh, D. Y. & Kemper, J. Bacteriophage P22-mediated specialized transduction in *Salmonella* typhimurium: identification of different types of specialized transducing particles. *J. Virol.* **27,** 535–550 (1978).

30. Wu, H., Sampson, L., Parr, R. & Casjens, S. The DNA site utilized by bacteriophage P22 for initiation of DNA packaging. *Mol. Microbiol.* **45,** 1631–1646 (2002).

31. Martínez-Rubio, R. *et al.* Phage-inducible islands in the Gram-positive cocci. *ISME J* **11,** 1029–1042 (2017).

32. Tsao, Y.-F. *et al.* Phage Morons play an important role in *Pseudomonas aeruginosa* phenotypes. *J. Bacteriol.* **200,** (2018).

33. Fillol-Salom, A. *et al.* Bacteriophages benefit from generalized transduction. *PLoS Pathog.* 15, e1007888 (2019).

34. Humphrey, S. *et al.* Redefining mobility in bacterial genetics: Chromosomal mobility via lateral transduction exceeds that of classical mobile genetic elements. *Nat. Commun.* (2nd revision).

35. Willard, M. & Echols, H. Role of bacteriophage DNA replication in lambda-dg escape synthesis. *J. Mol. Biol.* **32,** 37–46 (1968).

36. Imae, Y. & Fukasawa, T. Regional replication of the bacterial chromosome induced by derepression of prophage lambda. *J. Mol. Biol.* **54,** 585–597 (1970).

37. Osterhout, R. E., Figueroa, I. A., Keasling, J. D. & Arkin, A. P. Global analysis of host response to induction of a latent bacteriophage. *BMC Microbiol.* **7,** 82 (2007).

38. Datsenko, K. A. & Wanner, B. L. One-step inactivation of chromosomal genes in *Escherichia coli* K-12 using PCR products. *Proc. Natl. Acad. Sci. U.S.A.* **97,** 6640–6645 (2000).

39. Ubeda, C. *et al.* SaPI mutations affecting replication and transfer and enabling autonomous replication in the absence of helper phage. *Mol. Microbiol.* **67,** 493–503 (2008).

40. Nesin, M. *et al.* Cloning and nucleotide sequence of a chromosomally encoded tetracycline resistance determinant, *tet*A(M), from a pathogenic, methicillin-resistant

strain of Staphylococcus aureus. *Antimicrob. Agents Chemother.* **34,** 2273–2276 (1990).

41. Li, H. *et al.* The Sequence alignment/map format and SAMtools. *Bioinformatics* **25,** 2078–2079 (2009).
42. Quinlan, A. R. & Hall, I. M. BEDTools: a flexible suite of utilities for comparing genomic features. *Bioinformatics* **26,** 841–842 (2010).
43. Bankevich, A. *et al.* SPAdes: a new genome assembly algorithm and its applications to single-cell sequencing. *J. Comput. Biol.* **19,** 455–477 (2012).
44. Bolger, A. M., Lohse, M. & Usadel, B. Trimmomatic: a flexible trimmer for Illumina sequence data. *Bioinformatics* **30,** 2114–2120 (2014).
45. Förstner, K. U., Vogel, J. & Sharma, C. M. READemption-a tool for the computational analysis of deep-sequencing-based transcriptome data. *Bioinformatics* **30,** 3421–3423 (2014).
46. Livak, K. J. & T. D. Schmittgen. Analysis of relative gene expression data using real-time quantitative PCR and the 2(-Delta Delta C(T)) method. Methods **25**, 402–408 (2001).

Acknowledgements

This work was supported in part by the Singapore Ministry of Education MOE2017-T2-2-163 and MOE2019-T2-2-162 to J.C.; and by MR/M003876/1, MR/V000772/1 and MR/S00940X/1 from the Medical Research Council (UK), BB/N002873/1, BB/V002376/1 and BB/S003835/1 from the Biotechnology and Biological Sciences Research Council (BBSRC, UK), ERC-ADG-2014 Proposal n° 670932 Dut-signal (from EU), to J.R.P; and Wellcome Trust 201531/Z/16/Z to J.R.P.

Author Contributions: J.C. and J.R.P. conceived the study. A.F-S, S.H. and Y.N.C., conducted the experiments. R.B. performed the genomic and transcriptomic analyses. J.C. and J.R.P. wrote the manuscript.

Competing interests: Authors declare no competing interests.

Materials and correspondence: J.C and J.R.P.

Figure legends

Figure 1. The life cycle of temperate prophages after induction.

a, Representation of the classical ERP (excision, replication and packaging) model for prophage induction. **b,** The P22 tsc_2*29* heat-inducible mutant follows the ERP cycle. c, Representation of the RPE (replication, packaging and excision) model. In red, phage genome; in blue, chromosomal DNA.

Figure 2. Transcriptomic profile of P22 after prophage induction or phage infection.

Expression analysis of the early, middle and late genes from phages P22 and P22 tsc_2*29* for the positive (top) and the negative (bottom) DNA strands. For analysis of phage induction, lysogenic strains carrying phage P22 or P22 tsc_2*29* were induced (using mitomycin C or temperature-shift, respectively). For analysis of phage infection, the non-lysogenic LT2 strain was infected with P22. Samples were analyzed without induction or before infection (time 0, red), or at 30 min (early genes, cyan), 60 min (green) or 90 min (late genes, blue) following prophage induction or phage infection. Experiments were performed in triplicate. Error bars indicate standard deviation. Expression was normalized by the number of aligned reads.

Figure 3. Phage P22 and ES18 replicate *in situ* before excision.

Relative abundance of phage genomic DNA and the chromosomal regions proximal to where they integrate for P22 **(a)**, P22 tsc_2*29* **(b)**, P22 Δ*int* **(c)**, P22 Δ*xis* **(d)**, P22 Δ*pri* **(e)** or ES18 **(f)** is represented. Samples were analysed at 0 (red), 30 (cyan), 60 (green), and 90 min (blue) after induction of P22 prophage or at 0 (red), 60 (cyan), 90 (green), and 120 min (blue) after induction of ES18 (using mitomycin C or temperature-shift, as appropriate). Relative coverage is the DNA relative to the average bacterial genomic coverage (excluding phages).

748 **Figure 4. P22 and ES18 engages in lateral transduction, transferring large metameric**
749 **spans of the bacterial chromosome at high frequencies.**

750 **a,** The transfer of tetracycline (*tet*A) markers located upstream (*tet*A^{R}) or downstream of the
751 P22 *att*B site, in twelve successive capsid headfuls (*tet*A$^{"n"}$), was tested following P22
752 prophage induction (Ind) or P22 infection (Inf). **b,** The transfer of *tet*A markers located
753 upstream (*tet*A^{R}) or downstream of the P22 *att*B site, in ten successive capsid headfuls
754 (*tet*A$^{"n"}$), was tested after ES18 induction or ES18 infection. **c,** A P22 lysogen was mitomycin
755 C-induced and the resulting phage particles purified. The DNA from the phage particles was
756 extracted and sequenced. The coverage of chromosomal DNA is represented. **d,** Zoom of
757 the region encompassing lateral transduction is visualized, displaying a successive
758 'stepdown' pattern in DNA packaging efficiency for each consecutive headful. Transduction
759 units (TrU) per milliliter were normalized by PFU per milliliter and represented as the log TrU
760 of an average phage titre (1 x 10^{9} PFU). Error bars indicate standard deviation from the
761 mean of three independent experiments. For all panels, values are means (n = 3
762 independent samples). An unpaired two-sided t test was performed to compare mean
763 differences between infection and induction in each marker. Adjusted p values were as
764 follows: *ns*>0.05; *p≤0.05; **p≤0.01; ***p≤0.001; ****p≤0.0001. The exact statistical values for
765 each of the conditions tested are listed on Table S1.

766

767 **Figure 5. Effect of early or delayed excision on lateral transduction and phage**
768 **formation.**

769 The lysogenic strain for phage P22 mutant Δ*int-xis,* carrying a plasmid expressing the *int* and
770 *xis* genes, was mitomycin C-induced to activate the prophage, and arabinose (0.02%) was
771 added at different time points after induction of the resident prophage to facilitate *int-xis*
772 expression *in trans*. (-): no arabinose added. Lysates were tested for transduction of the
773 tetracycline (*tet*A) marker (colony forming units per milliltre: CFU/mL) **(a)** and to determine
774 the phage titre (plaque forming units per milliltre: PFU/mL) **(b)**. Error bars indicate standard

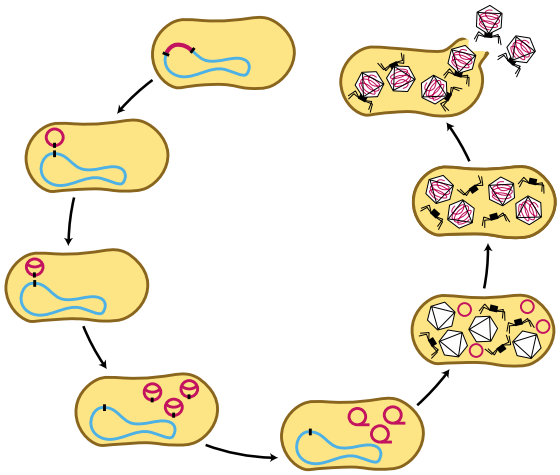
775 deviation from the mean of three independent experiments. For all panels, values are means
776 (n = 3 independent samples). A one-way ANOVA with Dunnett's multiple comparisons test
777 was performed to compare time 0 against the other timepoints. Adjusted p values were as
778 follows: *ns*>0.05; *p≤0.05; **p≤0.01; ***p≤0.001; ****p≤0.0001. The exact statistical values for
779 each of the conditions tested are listed in Table S1.

780

781

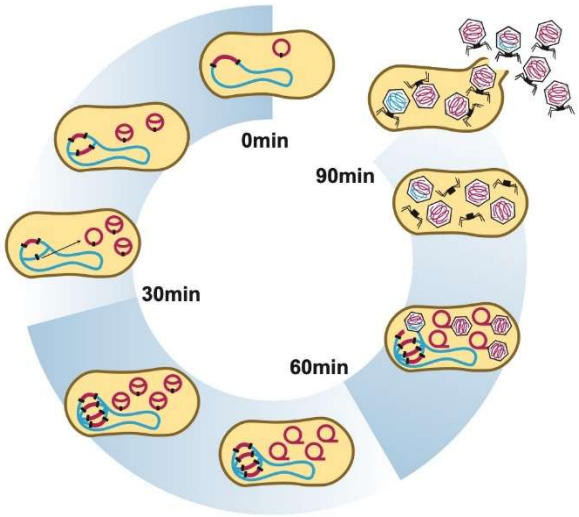
782

a



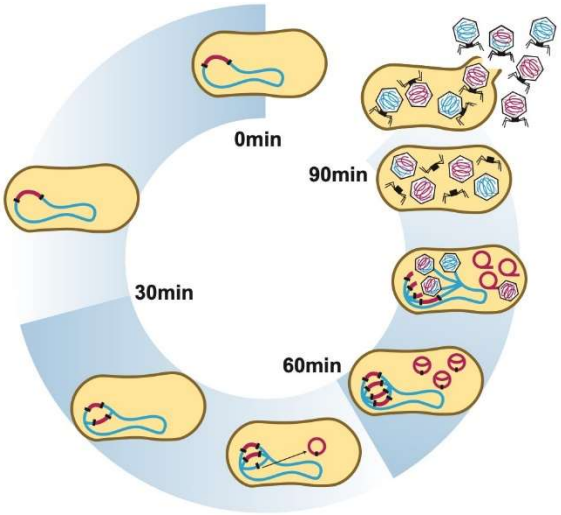
The classical ERP cycle

b

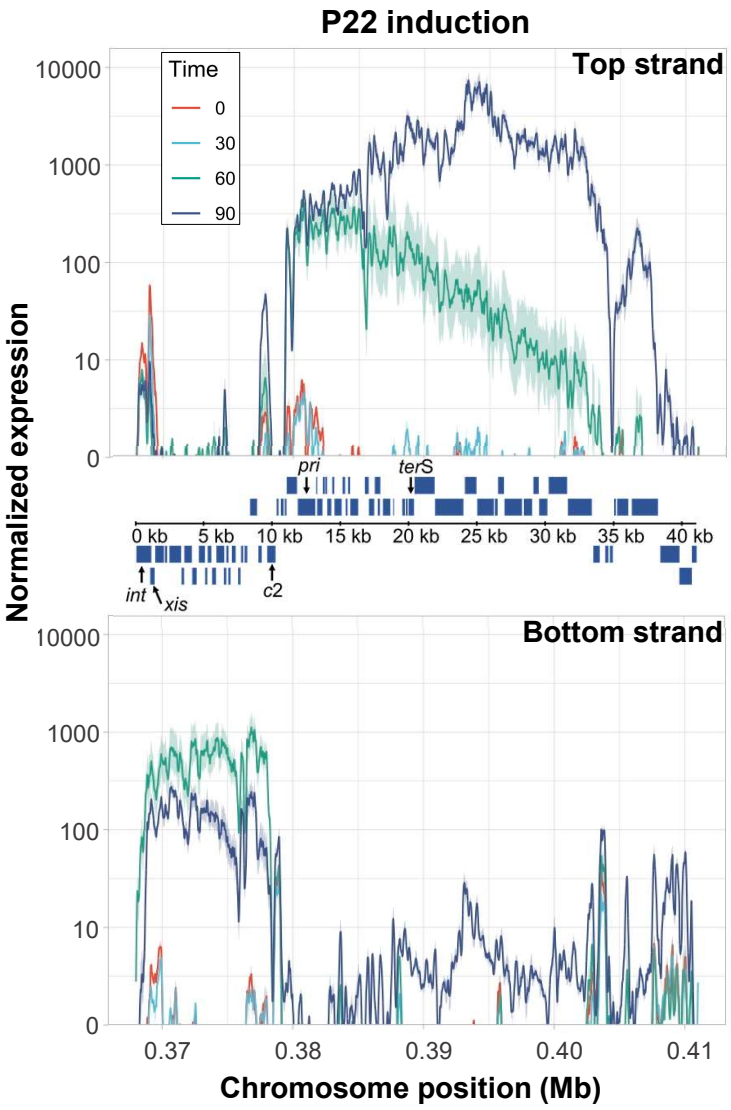


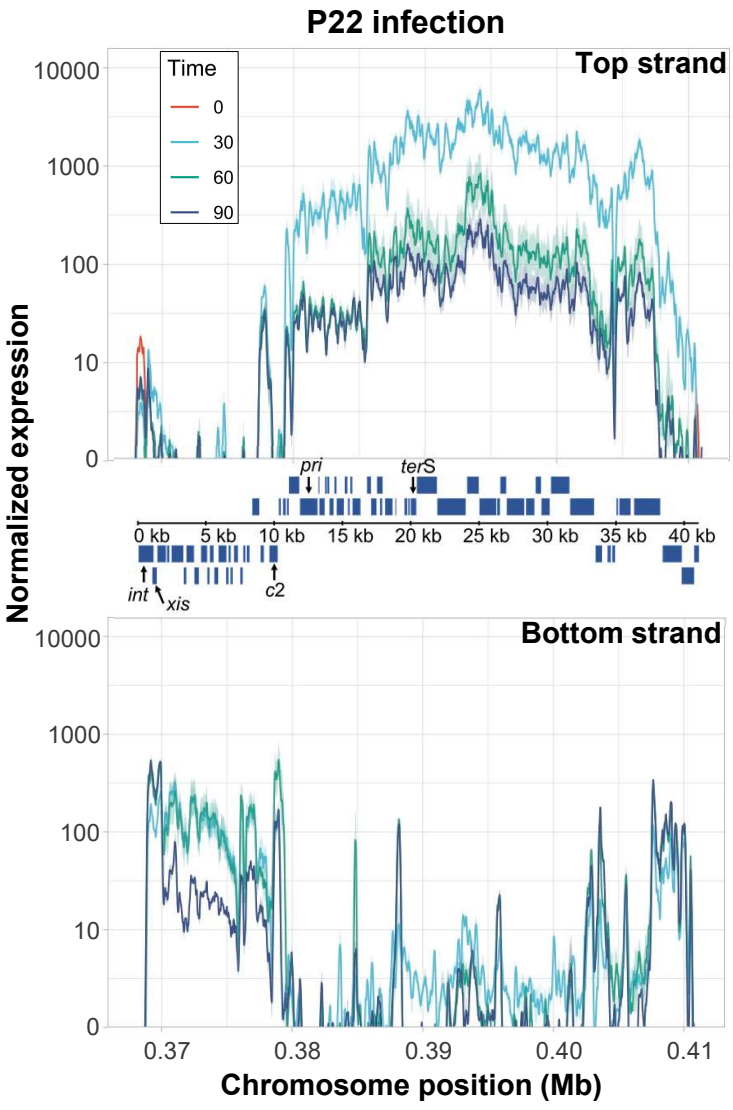
P22 tsc_2*29* heat-inducible mutant

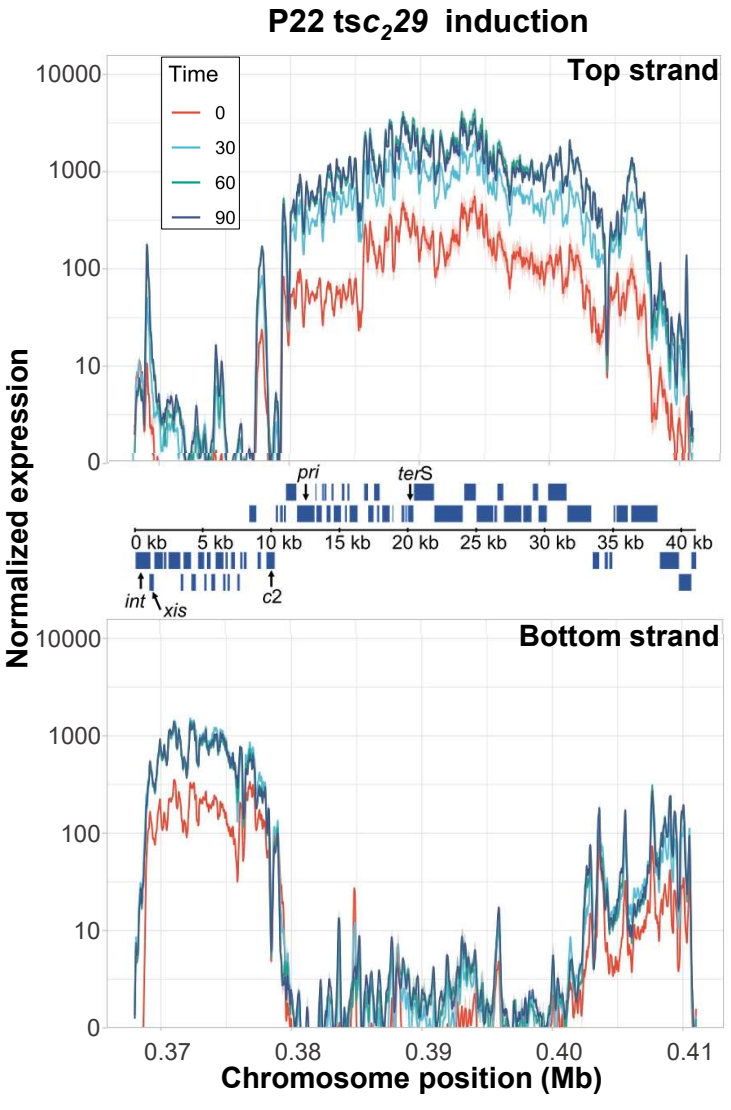
c

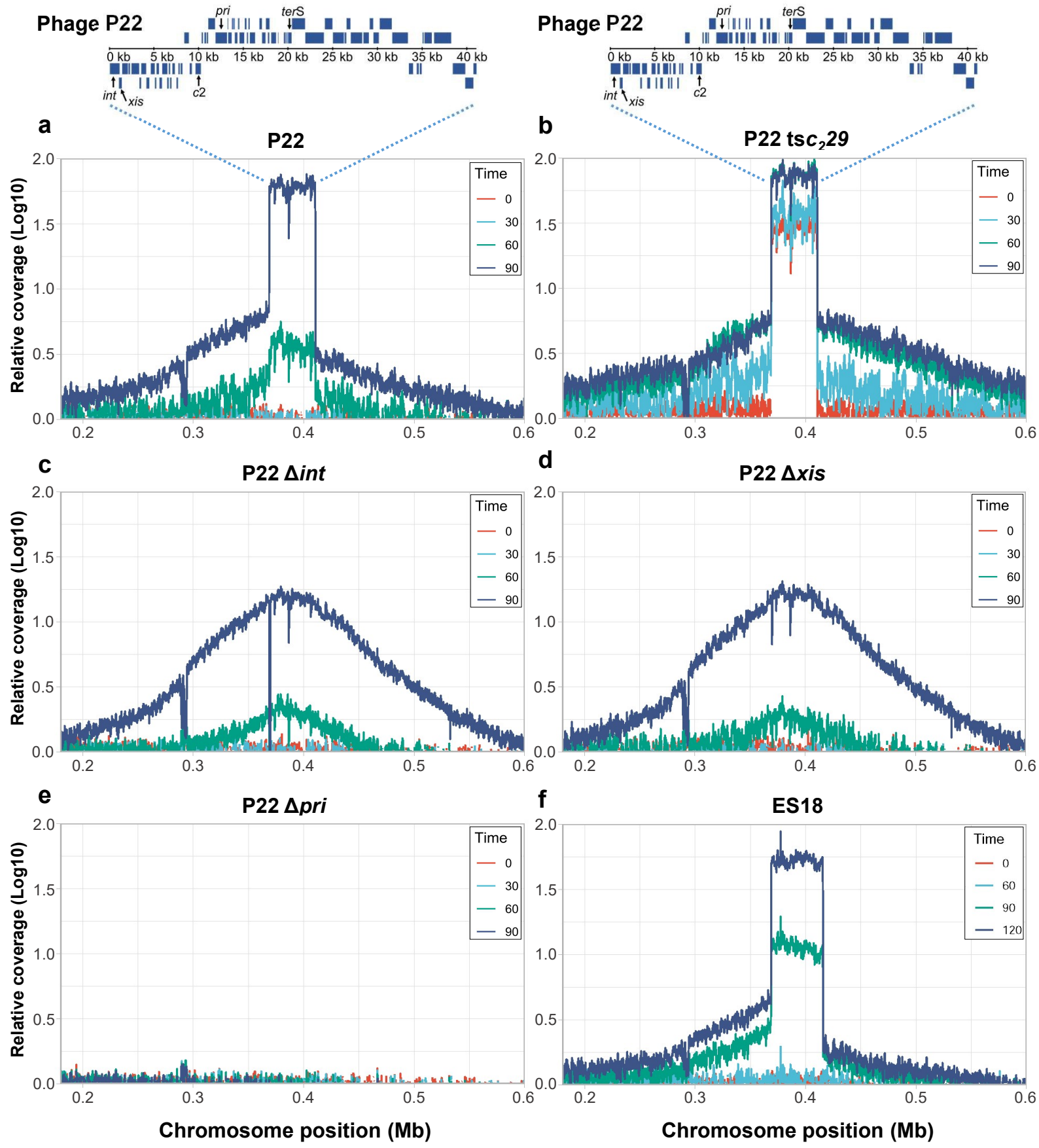


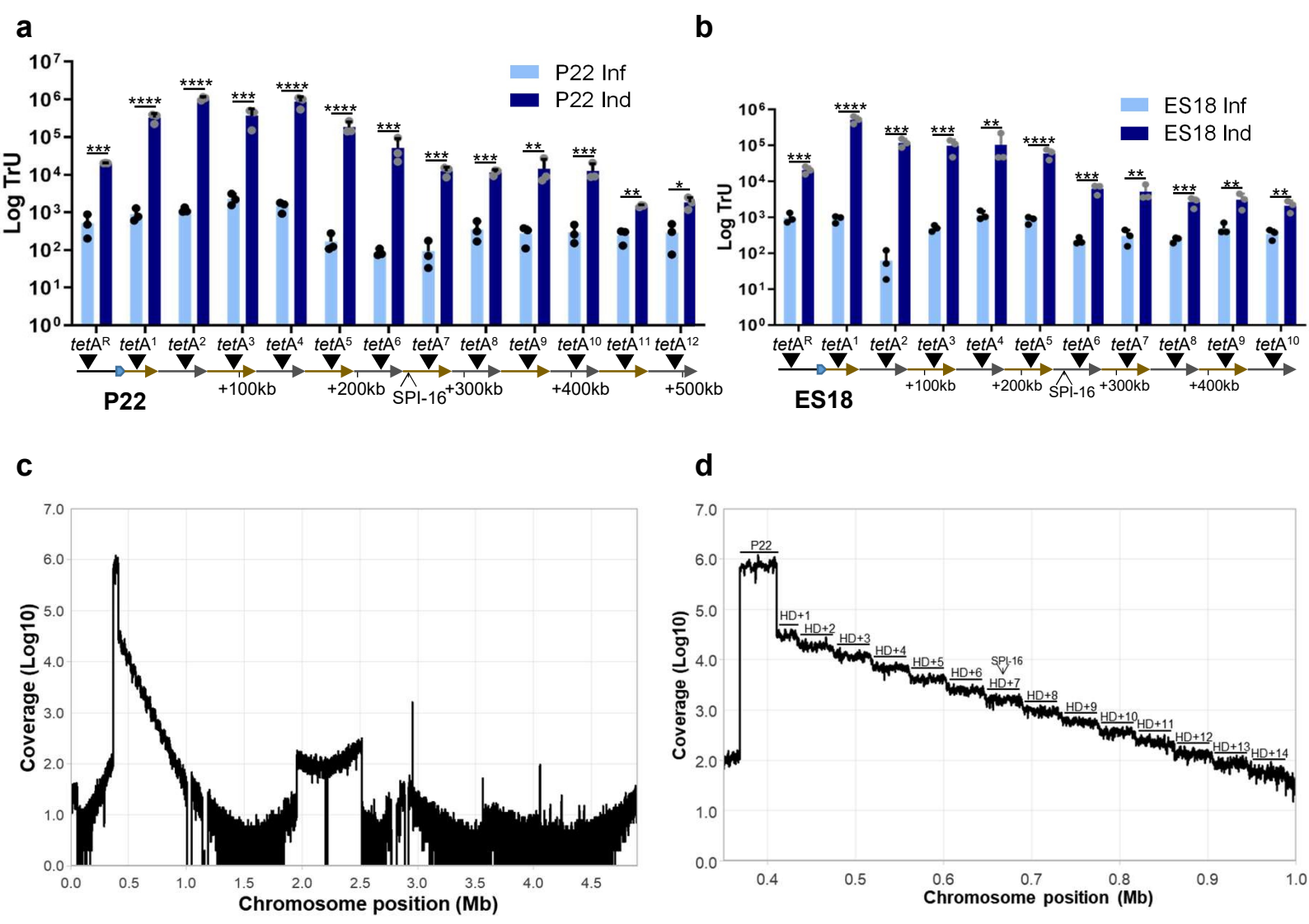
The RPE cycle


P22 induction
Top strand
Time
0
30
60
90
Normalized expression
10000
1000
100
10
0
pri
terS
0 kb
5 kb
10 kb
15 kb
20 kb
25 kb
30 kb
35 kb
40 kb
int
xis
c2
Bottom strand
0.37
0.38
0.39
0.40
0.41
Chromosome position (Mb)


P22 infection
Top strand
Time
0
30
60
90
Normalized expression
10000
1000
100
10
0
pri
terS
0 kb
5 kb
10 kb
15 kb
20 kb
25 kb
30 kb
35 kb
40 kb
int
xis
c2
Bottom strand
0.37
0.38
0.39
0.40
0.41
Chromosome position (Mb)


P22 tsc2 29 induction
Top strand
Time
0
30
60
90
Normalized expression
10000
1000
100
10
0
pri
terS
0 kb
5 kb
10 kb
15 kb
20 kb
25 kb
30 kb
35 kb
40 kb
int
xis
c2
Bottom strand
0.37
0.38
0.39
0.40
0.41
Chromosome position (Mb)

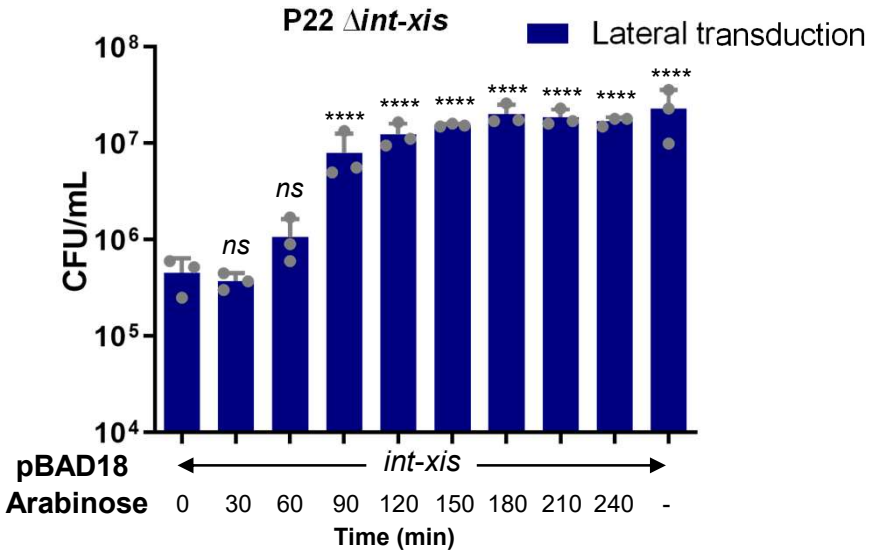

Phage P22
pri
terS
0 kb
5 kb
10 kb
15 kb
20 kb
25 kb
30 kb
35 kb
40 kb
int
xis
c2
a
P22
b
P22 tsc2 29
c
P22 Δint
d
P22 Δxis
e
P22 Δpri
f
ES18
Time
0
30
60
90
120
Relative coverage (Log10)
0.0
0.5
1.0
1.5
2.0
0.2
0.3
0.4
0.5
0.6
Chromosome position (Mb)


a
P22 Inf
P22 Ind
Log TrU
tetA^R tetA^1 tetA^2 tetA^3 tetA^4 tetA^5 tetA^6 tetA^7 tetA^8 tetA^9 tetA^10 tetA^11 tetA^12
P22
+100kb
+200kb
SPI-16
+300kb
+400kb
+500kb
b
ES18 Inf
ES18 Ind
Log TrU
tetA^R tetA^1 tetA^2 tetA^3 tetA^4 tetA^5 tetA^6 tetA^7 tetA^8 tetA^9 tetA^10
ES18
+100kb
+200kb
SPI-16
+300kb
+400kb

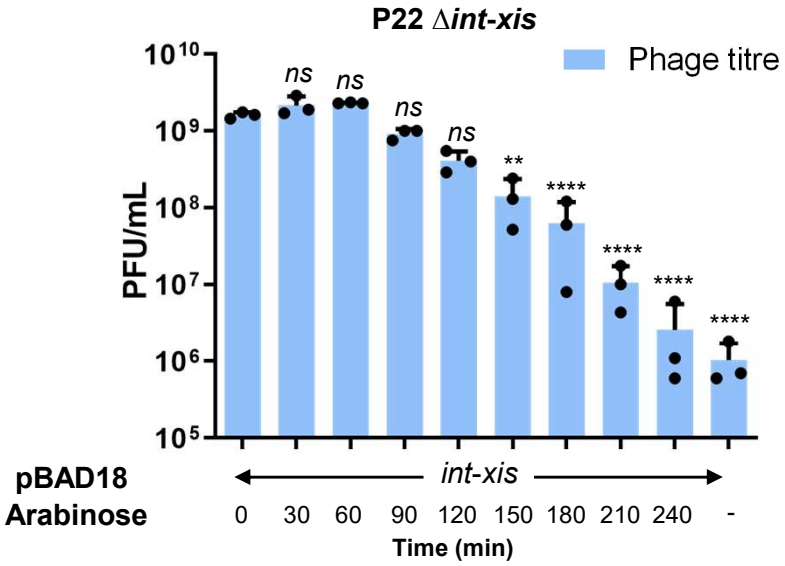
c
Coverage (Log10)
Chromosome position (Mb)

d
P22
HD+1
HD+2
HD+3
HD+4
HD+5
HD+6
SPI-16
HD+7
HD+8
HD+9
HD+10
HD+11
HD+12
HD+13
HD+14
Coverage (Log10)
Chromosome position (Mb)

a


P22 Δint-xis
Lateral transduction
CFU/mL
10^8
10^7
10^6
10^5
10^4
ns
ns
****
****
****
****
****
****
****
pBAD18
int-xis
Arabinose
0 30 60 90 120 150 180 210 240 -
Time (min)

b


P22 Δint-xis
Phage titre
PFU/mL
10^10
10^9
10^8
10^7
10^6
10^5
ns
ns
ns
ns
**
****
****
****
****
pBAD18
int-xis
Arabinose
0 30 60 90 120 150 180 210 240 -
Time (min)

Supplementary Tables.

Table S1. Statistical values.

Figure 4a	*p* value
HDR	0.0009
HD+1	< 0.0001
HD+2	< 0.0001
HD+3	0.0003
HD+4	< 0.0001
HD+5	< 0.0001
HD+6	0.0002
HD+7	0.0006
HD+8	0.0006
HD+9	0.0024
HD+10	0.0009
HD+11	0.0029
HD+12	0.0266
Figure 4b	***p* value**
HDR	0.0002
HD+1	< 0.0001
HD+2	0.0002
HD+3	0.0001
HD+4	0.0014
HD+5	< 0.0001
HD+6	0.0001
HD+7	0.0023
HD+8	0.0005
HD+9	0.0081
HD+10	0.0041

Figure 5a. Lateral transfer	*p* value
0-30	0.9974
0-60	0.0899
0-90	< 0.0001
0-120	< 0.0001
0-150	< 0.0001
0-180	< 0.0001
0-210	< 0.0001
0-240	< 0.0001
0- -	< 0.0001
Figure 5b. Phage titre	***p* value**
0-30	0.9975
0-60	0.9920
0-90	0.9101
0-120	0.1489
0-150	0.0017

0-180	< 0.0001
0-210	< 0.0001
0-240	< 0.0001
0- -	< 0.0001

Figure S5. qPCR EXCISION	***p* value**
P22 0-30	>0.9999
P22 0-60	0,1118
P22 0-90	0,0405
P22 ts 0-30	0,1916
P22 ts 0-60	0,6757
P22 ts 0-90	>0.9999
P22 Δ*pri* 0-30	>0.9999
P22 Δ*pri* 0-60	0,7658
P22 Δ*pri* 0-90	0,2902
ES18 0-60	0,6209
ES18 0-90	0,0258
ES18 0-120	0,0033

Figure S5. qPCR CIRCULARISATION	**p value**
P22 0-30	>0.9999
P22 0-60	0,5923
P22 0-90	<0.0001
P22 ts 0-30	0,9749
P22 ts 0-60	0,3107
P22 ts 0-90	0,8334
ES18 0-60	0,9989
ES18 0-90	0,0003
ES18 0-120	<0.0001

Figure S7	***p* value**
HD+1	0.1760
HD+2	0.2911
HD+3	0.0741
HD+4	0.8390
HD+5	0.1275
HD+6	0.4479
HD+7	0.5348
HD+8	0.0677
HD+9	0.6282
HD+10	0.9924
HD+11	0.1713
HD+12	0.7911

Figure S8a	***p* value**
HD+1	0.0207
HD+2	0.0131
Figure S8b	***p* value**
HD+1	0.0013
HD+2	0.0009

Figure S9	***p* value**
HD+1	0.0008
HD+2	0.0023
HD+4	0.0082
*tet*M^{G}	0.9364

Figure S10. P22 LT	***p* value**
wt-Δ*int*	0.0003
wt-Δ*xis*	0.0002
wt-Δ*int-xis*	0.0002
Figure S10. P22 titre	***p* value**
wt-Δ*int*	< 0.0001
wt-Δ*xis*	< 0.0001
wt-Δ*int-xis*	< 0.0001

Figure S10. ES18 LT	***p* value**
wt-Δ*int*	0.0136
wt-Δ*xis*	0.0335
wt-Δ*int-xis*	0.0434
Figure S10. ES18 titre	***p* value**
wt-Δ*int*	< 0.0001
wt-Δ*xis*	< 0.0001
wt-Δ*int-xis*	< 0.0001

Table S2. Strains used in this study.

Strain	Description	Reference
E. coli DC10B	K-12-derivative cloning strain; *dam*$^+$ *Ddcm DhsdRMS endA1 recA1*	[1]
VE18590	*E. faecalis* V583 derivative. Non-lysogenic, EfCIV583-negative.	[2]
VE18562	*E. faecalis* V583 derivative. fp1 lysogen, EfCIV583-negative.	[2]
JP18938	LT2 ΔFels-1 ΔGifsy-2 ΔGifsy-1 ΔFels-2	This work
JP22117	SV1208 ΔFels-1	This work
JP18983	JP18938 P22 lysogen	This work
JP18985	JP18938 ES18 lysogen	This work
JP22119	JP22117 P22 tsc_2*29* lysogen	This work
JP20460	JP18938 Δ*rfb*P-*rfb*B::*Km*R	This work
JP20590	JP18938 P22 lysogen Δ*int*	This work
JP20591	JP18938 P22 lysogen Δ*xis*	This work
JP20592	JP18938 P22 lysogen Δ*int-xis*	This work
JP20593	JP18938 P22 lysogen Δ*orf12*	This work
JP20595	JP18938 ES18 lysogen Δ*int*	This work
JP20596	JP18938 ES18 lysogen Δ*xis*	This work
JP20597	JP18938 ES18 lysogen Δ*int-xis*	This work
JP19020	JP18938 Δ*att*B P22	This work
JP22118	JP22117 Δ*att*B P22	This work
JP19086	JP19020 *gpt*ΩTetA (6 kb upstream P22 *att*B)	This work
JP19087	JP19020 STM0331ΩTetA (6 kb downstream P22 *att*B, HF1)	This work
JP19088	JP19020 *prp*RΩTetA (47 kb downstream P22 *att*B, HF2)	This work
JP19089	JP19020 *mal*ZΩTetA (88 kb downstream P22 *att*B, HF3)	This work
JP19090	JP19020 *yaj*GΩTetA (130 kb downstream P22 *att*B, HF4)	This work
JP19091	JP19020 *yba*NΩTetA (170 kb downstream P22 *att*B, HF5)	This work
JP19092	JP19020 *ybb*VΩTetA (213 kb downstream P22 *att*B, HF6)	This work
JP19093	JP19020 STM0557ΩTetA (246 kb downstream P22 *att*B, HF7)	This work
JP19094	JP19020 *ahp*FΩTetA (304 kb downstream P22 *att*B, HF8)	This work
JP19095	JP19020 *ybe*LΩTetA (348 kb downstream P22 *att*B, HF9)	This work
JP19096	JP19020 STM0699ΩTetA (392 kb downstream P22 *att*B, HF10)	This work
JP19097	JP19020 *nei*ΩTetA (425 kb downstream P22 *att*B, HF11)	This work
JP19098	JP19020 *mod*FΩTetA (474 kb downstream P22 *att*B, HF12)	This work
JP20469	JP18983 *gpt*ΩTetA (6 kb upstream P22 *att*B)	This work
JP20470	JP18983 STM0331ΩTetA (6 kb downstream P22 *att*B, HF1)	This work
JP20471	JP18983 *prp*RΩTetA (47 kb downstream P22 *att*B, HF2)	This work
JP20472	JP18983 *mal*ZΩTetA (88 kb downstream P22 *att*B, HF3)	This work
JP20473	JP18983 *yaj*GΩTetA (130 kb downstream P22 *att*B, HF4)	This work
JP20474	JP18983 *yba*NΩTetA (170 kb downstream P22 *att*B, HF5)	This work
JP20475	JP18983 *ybb*VΩTetA (213 kb downstream P22 *att*B, HF6)	This work
JP20476	JP18983 STM0557ΩTetA (246 kb downstream P22 *att*B, HF7)	This work
JP20477	JP18983 *ahp*FΩTetA (304 kb downstream P22 *att*B, HF8)	This work
JP20478	JP18983 *ybe*LΩTetA (348 kb downstream P22 *att*B, HF9)	This work
JP20479	JP18983 STM0699ΩTetA (392 kb downstream P22 *att*B, HF10)	This work
JP20480	JP18983 *nei*ΩTetA (425 kb downstream P22 *att*B, HF11)	This work
JP20481	JP18983 *mod*FΩTetA (474 kb downstream P22 *att*B, HF12)	This work
JP21928	JP22118 *gpt*ΩTetA (6 kb downstream P22 *att*B)	This work
JP21929	JP22118 *prp*RΩTetA (47 kb downstream P22 *att*B)	This work
JP21922	JP22119 *gpt*ΩTetA (6 kb downstream P22 *att*B)	This work
JP21923	JP22119 *prp*RΩTetA (47 kb downstream P22 *att*B)	This work
JP20482	JP18985 *gpt*ΩTetA (6 kb upstream P22 *att*B)	This work
JP20483	JP18985 STM0331ΩTetA (6 kb downstream P22 *att*B, HF1)	This work
JP20484	JP18985 *prp*RΩTetA (47 kb downstream P22 *att*B, HF2)	This work
JP20485	JP18985 *mal*ZΩTetA (88 kb downstream P22 *att*B, HF3)	This work
JP20487	JP18985 *yba*NΩTetA (170 kb downstream P22 *att*B, HF4)	This work
JP20488	JP18985 *ybb*VΩTetA (213 kb downstream P22 *att*B, HF5)	This work
JP20489	JP18985 STM0557ΩTetA (246 kb downstream P22 *att*B, HF6)	This work
JP20490	JP18985 *ahp*FΩTetA (304 kb downstream P22 *att*B, HF7)	This work
JP20491	JP18985 *ybe*LΩTetA (348 kb downstream P22 *att*B, HF8)	This work
JP20493	JP18985 *nei*ΩTetA (425 kb downstream P22 *att*B, HF9)	This work
JP20494	JP18985 *mod*FΩTetA (474 kb downstream P22 *att*B, HF10)	This work
JP19438	JP20470 Δ*rfb*P-*rfb*B::*Km*R	This work
JP19439	JP20471 Δ*rfb*P-*rfb*B::*Km*R	This work
JP19440	JP20472 Δ*rfb*P-*rfb*B::*Km*R	This work
JP19441	JP20473 Δ*rfb*P-*rfb*B::*Km*R	This work

JP19442	JP20474 Δ*rfb*P-*rfb*B::*Km*R	This work
JP19443	JP20475 Δ*rfb*P-*rfb*B::*Km*R	This work
JP19444	JP20476 Δ*rfb*P-*rfb*B::*Km*R	This work
JP19445	JP20477 Δ*rfb*P-*rfb*B::*Km*R	This work
JP19446	JP20478 Δ*rfb*P-*rfb*B::*Km*R	This work
JP19447	JP20479 Δ*rfb*P-*rfb*B::*Km*R	This work
JP19448	JP20480 Δ*rfb*P-*rfb*B::*Km*R	This work
JP19449	JP20481 Δ*rfb*P-*rfb*B::*Km*R	This work
JP21422	JP19020 Cat marker 6 kb downstream P22 *att*B + TetA marker 6 kb upstream P22 *att*B	This work
JP21423	JP19020 Cat marker 6 kb downstream P22 *att*B + TetA marker 10 kb up downstream P22 *att*B	This work
JP21424	JP19020 Cat marker 6 kb downstream P22 *att*B + TetA marker 29 kb up downstream P22 *att*B	This work
JP21425	JP19020 Cat marker 6 kb downstream P22 *att*B + TetA marker 32 kb up downstream P22 *att*B	This work
JP21426	JP19020 Cat marker 10 kb downstream P22 *att*B + TetA marker 29 kb upstream P22 *att*B	This work
JP21427	JP19020 Cat marker 10 kb downstream P22 *att*B + TetA marker 32 kb upstream P22 *att*B	This work
JP21428	JP19020 Cat marker 15.6 kb downstream P22 *att*B + TetA marker 29 kb upstream P22 *att*B	This work
JP21429	JP19020 Cat marker 15.6 kb downstream P22 *att*B + TetA marker 32 kb upstream P22 *att*B	This work
JP21430	JP19020 Cat marker 29 kb downstream P22 *att*B + TetA marker 32 kb upstream P22 *att*B	This work
JP21431	JP18983 Cat marker 6 kb downstream P22 *att*B + TetA marker 6 kb upstream P22 *att*B	This work
JP21432	JP18983 Cat marker 6 kb downstream P22 *att*B + TetA marker 10 kb up downstream P22 *att*B	This work
JP21433	JP18983 Cat marker 6 kb downstream P22 *att*B + TetA marker 29 kb up downstream P22 *att*B	This work
JP21434	JP18983 Cat marker 6 kb downstream P22 *att*B + TetA marker 32 kb up downstream P22 *att*B	This work
JP21435	JP18983 Cat marker 10 kb downstream P22 *att*B + TetA marker 29 kb upstream P22 *att*B	This work
JP21436	JP18983 Cat marker 10 kb downstream P22 *att*B + TetA marker 32 kb upstream P22 *att*B	This work
JP21437	JP18983 Cat marker 15.6 kb downstream P22 *att*B + TetA marker 29 kb upstream P22 *att*B	This work
JP21438	JP18983 Cat marker 15.6 kb downstream P22 *att*B + TetA marker 32 kb upstream P22 *att*B	This work
JP21439	JP18983 Cat marker 29 kb downstream P22 *att*B + TetA marker 32 kb upstream P22 *att*B	This work
JP20600	JP20590 *prp*RΩTetA (47 kb downstream P22 *att*B, HF2)	This work
JP20601	JP20591 *prp*RΩTetA (47 kb downstream P22 *att*B, HF2)	This work
JP20602	JP20592 *prp*RΩTetA (47 kb downstream P22 *att*B, HF2)	This work
JP20605	JP20595 *prp*RΩTetA (47 kb downstream P22 *att*B, HF2)	This work
JP20606	JP20596 *prp*RΩTetA (47 kb downstream P22 *att*B, HF2)	This work
JP20607	JP20597 *prp*RΩTetA (47 kb downstream P22 *att*B, HF2)	This work
JP20757	JP20602 pJP2534	This work
JP21704	*E. coli* DC10B pJP2563	This work
JP21747	*E. coli* DC10B pJP2564	This work
JP21748	*E. coli* DC10B pJP2565	This work
JP21896	*E. coli* DC10B pJP2566	This work
JP21706	*E. coli* DC10B pJP2568	This work
JP21767	VE18590 *celA*Ω*tet*M (12.3 kb upstream of pp1 *att*B)	This work
JP21855	VE18590 EF0370Ω*tetM* (12.3 kb downstream of pp1 *att*B, HF1)	This work
JP22112	VE18590 EF0394Ω*tetM* (40.7 kb downstream of pp1 *att*B, HF2)	This work
JP22021	VE18590 EF0480Ω*tetM* (121.1 kb downstream of pp1 *att*B, HF4)	This work
JP21771	VE18590 EF2276Ω*tetM* (1.87 Mb downstream of pp1 *att*B)	This work
JP21768	VE18562 *celA*Ω*tetM* (12.3 kb upstream of pp1 *att*B)	This work
JP21856	VE18562 EF0370Ω*tetM* (12.3 kb downstream of pp1 *att*B, HF1)	This work
JP21857	VE18562 EF0394Ω*tetM* (40.7 kb downstream of pp1 *att*B, HF2)	This work
JP22110	VE18562 EF0480Ω*tetM* (121.1 kb downstream of pp1 *att*B, HF4)	This work

JP21772	VE18562 EF2276Ω*tetM* (1.87 Mb downstream of pp1 *att*B)	This work

Table S3. Oligonucleotides used in this study.

Mutagenesis	Primers	Sequence (5'-3')
LT2 ΔFels-1	**LT2-AFels1-1m**	GGGGCACTCCTGGGGCAGTAGATGCCAGTTGTTGATTCAG TATATCTACTGTGTAGGCTGGAGCTGCTTCG
	LT2-AFels1-2c	GGCATCATACTGTACACTGTCATATGCCATATATTTAAACGC TAAAAGGGCATATGAATATCCTCCTTA
LT2 ΔGifsy-2	**LT2-AGifsy2-13m**	CGCTGGAGTATACCTTGTTTAGCGATTTATTGAACCCCGATC ACACCTGTGTAGGCTGGAGCTGCTTCG
	LT2-AGifsy2-14c	GCAAATCGCGCTACGCAGAATGTTCATCTTTTCAGGCACAA ACGGCCGGTCCATATGAATATCCTCCTTAG
LT2 ΔGifsy-1	**LT2-AGifsy1-1m**	CAAGTAACGAGGCGACATCAAACCTTGAGTTATTAAATAAAT GGAGAATAGTGTGTAGGCTGGAGCTGCTTCG
	LT2-AGifsy1-2c	GTCCCTGATATGGGCGTGCAGGGTCGGTGAACTCCGTCAG GCTGAAGCATATGAATATCCTCCTTA
LT2 ΔFels-2	**LT2-AFels2-1m**	CTTCAAGCTCCATGCTGGTCGTAAATCCATTATCCGGGCTG ACAGAATGCTGTGTAGGCTGGAGCTGCTTCG
	LT2-AFels2-2c	TTCCTTGAGCATCTTCGGGCGGATCTCGGTAACGGGTGTGT TACCCAGAGCATATGAATATCCTCCTTA
LT2 Δ*att*B P22	**LT2-AattB-1m**	CCTTCTACCCCGTGATTCACCCGCGTGAACACACCCTTCTC ATGTGTAGGCTGGAGCTGCTTCG
	LT2-AattB-2c	GGATACTGCTTATGTTTTGCTAGTTGTGTACCCGAGAGTGTA CCCGGTCCATATGAATATCCTCCTTAG
LT2 Δ*rfb*P-*rfb*B P22	**LT2-ArfbP-1m**	TTTTACGCAGGCTAATTTATACAATTATTATTCAGTACTTCTC GGTAAGCTTGTGTAGGCTGGAGCTGCTTCG
	LT2-ArfbB-2c	TTTATTGGCAAATTAAATACCACATTAAATACGCCTTATGGA ATAGAAAACATATGAATATCCTCCTTA
***tet*A marker 6 kb upstream P22 *att*B**	**LT2-tetA-11m**	TCAGACACGATAAGTCTCCTTGGCGGTGGTCTGAAAAACGT TCTTACAGGCCACAGGGTTCGCTGTTAATCACTTTACTT
	LT2-tetA-12c	ACCCGCAGGCGGAGAAAGTGGTATTCTCAGTCGCATCTCGT AAGAGTTATCAATTCCGCTGGTTATCAAGAGGGTCATTA
***tet*A marker 6 kb downstream P22 *att*B**	**LT2-tetA-3m**	GGTTGCGCATTATTCACGGCGGCCGTGGCTAAAACGCCCT GCATCCCCGCGCGGTTAAGGCGCTGTTAATCACTTTACTT
	LT2-tetA-4c	AATGCCGTAGCGTTTGCCACCGTTCACAAGATATTGAACCA GTTTCATTGCAGTCTTCTTGGTTATCAAGAGGGTCATTA
***tet*A marker 47 kb downstream P22 *att*B**	**LT2-tetA-6m**	ATTGCATCATAAAAATACCCGCCTGGGTTTCCGGCGGGTAT ATTTATTCCTGGCAACCGGCGCTGTTAATCACTTTACTT
	LT2-tetA-7c	GCGTCCTGAATGCCTGATGGCGCTACGTTTACTGCAGGCC GTCATCCGGCAAAACGGATGGGTTATCAAGAGGGTCATTA
***tet*A marker 88 kb downstream P22 *att*B**	**LT2-tetA-9m**	GCGAGGGAAGACTTAGTTTACCCGCGATTTCCGCGACGGT ATGGATGAATCGTTGAGGCGCGCTGTTAATCACTTTACTT
	LT2-tetA-10c	CATTGATAAAAGGCTCGCGAATGCGAGCCTTTTTTATGCGT AAGGTGTTACGAACCACCTGGTTATCAAGAGGGTCATTA
***tet*A marker 130 kb downstream P22 *att*B**	**LT2-tetA-13m**	CGTAAATATTGACTTGACATAGGCATCTACAGACCCGGCTT CTGCCGGGTCTTGTTGTTGCGCTGTTAATCACTTTACTT
	LT2-tetA-14c	GCTGATATGTCTCAGGACACCAGTATTCACGATTTTATCAAG CAAAACGCCCGTTAATAGGGTTATCAAGAGGGTCATTA
***tet*A marker 170 kb downstream P22 *att*B**	**LT2-tetA-15m**	CTGCTGATTTTTATGTGGCGGATACCGGTGATTGATGAAAA GCAACAAAAGCGCTGAAGCCGCTGTTAATCACTTTACTT
	LT2-tetA-16c	TGTGCTCGAAAACGGTCGAATTTACTGGCTGTGAACGACAA TTGCAACAGCGATTCGTGTGGTTATCAAGAGGGTCATTA
***tet*A marker 213 kb downstream P22 *att*B**	**LT2-tetA-17m**	TCACTTTATATAAAAAGAAAGCAACGCAACGTATTGCTTCAG CTTAAAAATAATTATATCCGCTGTTAATCACTTTACTT
	LT2-tetA-18c	GATAACGTTGTTATGGGTTTAGCTATGAGGAACAAATAAATA TAAAATAAAGAATTAGTAGGTTATCAAGAGGGTCATTA
***tet*A marker 246 kb**	**LT2-tetA-19m**	TGTAGGAATCCCCGCCGCCCGTTACCCATTGGTGGCGGGG AACATTAATTATACATGAATCGCTGTTAATCACTTTACTT

downstream P22 *att*B	**LT2-tetA-20c**	CATGGGACGTTAGAACAGGGGCGAGGACAAATGAGAATATT ACGGAAATAATTAAATAACGGTTATCAAGAGGGTCATTA
***tet*A marker 304 kb**	**LT2-tetA-25m**	GCCTTTGATTATCTGATTCGCACCAAAATCGCATAAAAAGAA GTAAGCACACCTGCAAGGCGCTGTTAATCACTTTACTT
downstream P22 *att*B	**LT2-tetA-26c**	AAACACCGCAGGCCCGAATAGCTTACACTATCGGGCCATTT ACGATGGCCAGTTAACTGGGGTTATCAAGAGGGTCATTA
***tet*A marker 348 kb**	**LT2-tetA-27m**	GTGTGGCCACGATCAGTTCCAGCGCAGGCCGTTTGAGCCG TAAGGTTCATTATCGTGAGCCGCTGTTAATCACTTTACTT
downstream P22 *att*B	**LT2-tetA-28c**	GAAGAGATCCGCAAACTGGAAGCCCAACTGCACGCTTAACA TGGCGGACGGCAACCGTCCGGTTATCAAGAGGGTCATTA
***tet*A marker 392 kb**	**LT2-tetA-21m**	TGAGAAAGAAGCCGTTGAAATCGTTAGCGAAGTATTGAAAA ACGCCTGATGGGCGATATGCGCTGTTAATCACTTTACTT
downstream P22 *att*B	**LT2-tetA-22c**	AGGCCTGATAAGCGCAGCGCCGTTAATACAAAAAAGGAGC CGTAAGGCTCCTTTTTCTTCGGTTATCAAGAGGGTCATTA
***tet*A marker 425 kb**	**LT2-tetA-29m**	CGCATTGCCAGAAATAGCCGGAACCGACATCGGCGAGCGG CTATTGCCTGATGGCGCGACCGCTGTTAATCACTTTACTT
downstream P22 *att*B	**LT2-tetA-30c**	AGCAGTGGCCCGTTTTATATCAACCTATGCGCCCAAACAAC CTTTGTAGGGCTGATAAGCGGTTATCAAGAGGGTCATTA
***tet*A marker 474 kb**	**LT2-tetA-23m**	TATCGACCGTTATTATTATTCTTAATAAAAGGAGAGTGGTTC CAGAATGGCGCGCGGCGCCGCTGTTAATCACTTTACTT
downstream P22 *att*B	**LT2-tetA-24c**	AGGGCGAACGTTATAAGTACGTTTCCGGACGATGCAATAAT TAAATGTATTATCAGAATGGGTTATCAAGAGGGTCATTA
***cat* marker 6 kb**	**LT2-STM0331-cat-1m**	GGTTGCGCATTATTCACGGCGGCCGTGGCTAAAACGCCCT GCATCCCCGCGCGGTTAAGGGGCGCGCCTACCTGTGACGG
downstream P22 *att*B	**LT2-STM0331-cat-2c**	AATGCCGTAGCGTTTGCCACCGTTCACAAGATATTGAACCA GTTTCATTGCAGTCTTCTTGGAATAGGAACTTCATTTAAATG GC
***tet*A marker 10 kb**	**LT2-stbE-tetA-2c**	CTCCTGAGTTTTGATGGGAAATATTCAGGGATACGATCGTAT CCCTGAGGGGTTATCAAGAGGGTCATTA
downstream P22 *att*B	**LT2-stbE-tetA-1m**	ATCAGCTTAATGCTATTTTTGACAATGGTACATGCTGAGTCT GGCTTGCGCTGTTAATCACTTTACTT
***tet*A marker 29 kb**	**LT2-STM0352-tetA-1m**	CGTTTCCCTCTTTACCGCAGCGTGTCGGCCATTCCGCAACG CTGCCGCAGCGCTGTTAATCACTTTACTT
downstream P22 *att*B	**LT2-STM0352-tetA-2c**	CCCGTCAGGAACGCTTGACCTTTCCTTCGTTGTAACGCCTA GCCTTTGCCGGTTATCAAGAGGGTCATTA
***tet*A marker 32 kb**	**LT2-STM0355-tetA-1m**	CCGGTTTCCCGCCGCGCGAGAGGTAATCGTCAATGGCGAT CGGTCTGGCGCGCTGTTAATCACTTTACTT
downstream P22 *att*B	**LT2-STM0355-tetA-2c**	CTCACGCAAAGAAAAGCGAAGCGTGGCTAGCGTATCGCGA CCGGCCTGTGGTTATCAAGAGGGTCATTA
***cat* marker 10 kb**	**LT2-stbE-cat-1m**	ATCAGCTTAATGCTATTTTTGACAATGGTACATGCTGAGTCT GGCTTGGGCGCGCCTACCTGTGACGG
downstream P22 *att*B	**LT2-stbE-cat-2c**	CTCCTGAGTTTTGATGGGAAATATTCAGGGATACGATCGTAT CCCTGAGGGGAATAGGAACTTCATTTAAATGGC
***cat* marker 15.6 kb**	**LT2-stbB-cat-1m**	CAACTCCCTAGCGATTGAAAATGGTCTGGCGTTTCAACGCC AGACCGTAGGGCGCGCCTACCTGTGACGG
downstream P22 *att*B	**LT2-stbB-cat-2c**	GGGACAGTCGCTGCCACCCTTCAATACGCCGTTTCGTATAA ATAATTGTCGGAATAGGAACTTCATTTAAATGGC
***cat* marker 29 kb**	**LT2-STM0352-cat-1m**	CGTTTCCCTCTTTACCGCAGCGTGTCGGCCATTCCGCAACG CTGCCGCAGGGCGCGCCTACCTGTGACGG
downstream P22 *att*B	**LT2-STM0352-cat-2c**	CCCGTCAGGAACGCTTGACCTTTCCTTCGTTGTAACGCCTA GCCTTTGCCGGAATAGGAACTTCATTTAAATGGC
P22 Δ*int* (same primers used for ES18 Δ*int)*	**P22-Aint-3m**	CCCGCTCGTTTTAATGCTGCCCTCCATGCAGTATTAGCGTC ATAGTGTGTAGGCTGGAGCTGCTTCG
	P22-Aint-4c	GAGGAGAAGGCGCATAAGAAGTCGCTGGATGATGACAAGA GTCGGGGTCCATATGAATATCCTCCTTAG
P22 Δ*xis*	**P22-Axis-1m**	ATGTCATCACCCGCGCTCACCTGGACAGTATGCAGCGGAG ATTGAAGTGCTGTGTAGGCTGGAGCTGCTTCG

	P22-Axis-2c	GAAACAGCGGAGTAAACATGGAATCACACAGCCTCACACTT GATGAGGCCGGTCCATATGAATATCCTCCTTAG
P22 Δ*int-xis*	**P22-Aint-3m**	CCCGCTCGTTTTAATGCTGCCCTCCATGCAGTATTAGCGTC ATAGTGTGTAGGCTGGAGCTGCTTCG
	P22-Axis-2c	GAAACAGCGGAGTAAACATGGAATCACACAGCCTCACACTT GATGAGGCCGGTCCATATGAATATCCTCCTTAG
P22 Δ*orf12*	**P22-Aorf12-1m**	GGTGGCTTGCTGATTGGCGGATTAACACCAACCGCCAGTG ACGTTCTGGCTGTGTAGGCTGGAGCTGCTTCG
	P22-Aorf12-2c	GCGGCTTCCTGATGGATGACAGGCGCTTTACAAGCTCGTCC ATCGCTCTGGGTCCATATGAATATCCTCCTTAG
ES18 Δ*xis*	**ES18-Axis-1m**	TATGCCATCACCCGCGCTCACGGCGACAGTATGCATCGGA GACTGAAGAGTGTGTAGGCTGGAGCTGCTTCG
	ES18-Axis-2c	AGCAATAACAATCCTCGCACTCGCGGGGATTTCTTTTATCC GGAGTAACCGGTCCATATGAATATCCTCCTTAG
ES18 Δ*int-xis*	**P22-Aint-3m**	CCCGCTCGTTTTAATGCTGCCCTCCATGCAGTATTAGCGTC ATAGTGTGTAGGCTGGAGCTGCTTCG
	ES18-Axis-2c	AGCAATAACAATCCTCGCACTCGCGGGGATTTCTTTTATCC GGAGTAACCGGTCCATATGAATATCCTCCTTAG

Excision	**Primers**	**Sequence (5'-3')**
P22 and ES18	**LT2-attB-1m**	TCAGCACGCAGAAATTACATG
	LT2-attB-2c	ACGGAATCATTAACATGATGG

Circularisation	**Primers**	**Sequence (5'-3')**
P22	**P22-gtrA-4m**	GTTTTGATCGATACAAGCGATC
	P22-int-7c	CCTGACTGAACATGCTCGAC
ES18	**ES18-orf33-1m**	TCATCAACAGTGCGACAGATG
	P22-int-7c	CCTGACTGAACATGCTCGAC

Housekeeping	**Primers**	**Sequence (5'-3')**
P22 and ES18	**LT2-rapA-1m**	CGCTGAGCTGGCGGTTGAAGG
	LT2-rapA-2c	TGCCGCGAGCAACATGAAGCG

Plasmid	Primers	Sequence (5'-3')	Comment
pBAD18			
pJP2534	**P22-int-5mS**	ACGCGTCGACCAAATACTTACGTATTATTCGTGCC	
	P22-xis-4cE	CCGGAATTCATTCTACGACATCGCTAACGC	
pBT2bgal			
pJP2563	**pp1-HF-1_FB**	AGTAGGATCCCAAAAGTAGGGGCCTTTTCTGCACCTTTTACAGC	*celA* left flank
	pp1-tetM_HF-1_R	CTCAAATTGCGAGATTTGGGTTGCCTTTGTTTCTTGATCAAATTTGAACAAAGGACTGAAACGATATGTCAATTTTGAAAAATG	
	tetM-F	GATCAAGAAACAAAGGCAACCCAAATCTCGCAATTTGAG	*tetM* cassette
	tetM-RS	GTCAGTCGACGATCTTGTATCATTACTCCATGTATCTATTGATG	
	pp1-HF-1_FB	AGTAGGATCCCAAAAGTAGGGGCCTTTTCTGCACCTTTTACAGC	*celA* left flank-*tetM* fusion
	tetM-RS	GTCAGTCGACGATCTTGTATCATTACTCCATGTATCTATTGATG	
	pp1-HF-1_FS	CATTTTTCAAAATTGACATATCGTTTCAGTCCTTTGTTCAAATTTGTCGACTTATACGTTTTGTGCTTCGACTTTTTCAAGGGTTTCTTC	*celA* right flank
	pp1-HF-1_RH	TGCAAAGCTTGTTTTCATTTTGTTTATGTCATCTGAAGTCAAAGATGCG	
pJP2564	**pp1-HF1_FB**	ATGAGGATCCGGCTACAACCAATTATTAGCTGACGATTATGTG	EF0370 left flank
	pp1-tetM_HF1-R	CTCAAATTGCGAGATTTGGGTTGCCTTTGTTTCTTGATCTTAAATTGCTGTTAAATTAGGGTTATTGATATTTTTAAAATAAAAATC	
	tetM-F	GATCAAGAAACAAAGGCAACCCAAATCTCGCAATTTGAG	*tetM* cassette
	tetM-RS	GTCAGTCGACGATCTTGTATCATTACTCCATGTATCTATTGATG	
	pp1-HF1_FB	ATGAGGATCCGGCTACAACCAATTATTAGCTGACGATTATGTG	EF0370 left flank-*tetM* fusion
	tetM-RS	GTCAGTCGACGATCTTGTATCATTACTCCATGTATCTATTGATG	
	pp1-HF1_FX	AAATATCAATAACCCTAATTTAACAGCAATTTAATCTAGAATTAAACAATCACTAAACAGAGGCTTGTCGACAG	EF0370 right flank
	pp1-HF1_RNh	GTCTGCTAGCTGGCGCAAAATGTTCATTATCTTGTGAAAAAAC	
pJP2565	**pp1-HF2_FB**	TGCAGGATCCACAACAATGCTAGATGCAGTTTTAGATGCGGACTC	EF0370 left flank
	pp1-tetM_HF2-R	CTCAAATTGCGAGATTTGGGTTGCCTTTGTTTCTTGATCTTAGGCTGAGTGTCCTACGATTGTGCTACCTGAGTAACC	
	tetM-F	GATCAAGAAACAAAGGCAACCCAAATCTCGCAATTTGAG	*tetM* cassette
	tetM-RS	GTCAGTCGACGATCTTGTATCATTACTCCATGTATCTATTGATG	
	pp1-HF2_FB	TGCAGGATCCACAACAATGCTAGATGCAGTTTTAGATGCGGACTC	EF0370 left flank-*tetM* fusion
	tetM-RS	GTCAGTCGACGATCTTGTATCATTACTCCATGTATCTATTGATG	

	pp1-HF2_FS	CTCAGGTAGCACAATCGTAGGACACTCAGCCTAAGTCGACTCAGCAATGATAAAAATAGACGTAAGCAGCTTC	EF0370 right flank
	pp1-HF2_RNh	ATGTGCTAGCATCATCAAATTGCAAATAACGGCAACCTCTCTC	
pJP2566	**pp1-HF4_FB**	ATGTGGATCCCATTTTAGTTAAATCAGTAATTTTCAATATCGAGGG	EF0480 left flank
	pp1-HF4_RS	GAAGCTATCTTAAAATTTAAAATTAACTAAGTCGACCTAAAAAAAGCCCCTTTCCACTTTTTCTG	
	tetM-FS	GTACGTCGACGATCAAGAAACAAAGGCAACCCAAATCTCGCAATTTGAG	*tetM* cassette
	tetM-RS	GTCAGTCGACGATCTTGTATCATTACTCCATGTATCTATTGATG	
	pp1-HF4_FS	CAGAAAAAGTGGAAAGGGGCTTTTTTTAGGTCGACTTAGTTAATTTTAAATTTTAAGATAGCTTC	EF0480 right flank
	pp1-HF4_RH	GTCTAAGCTTCTGATTAAAACTTTATTATGATGTCATAGTGAAG	
pJP2568	**2196839_FB**	ATGTGGATCCGAAATAAGCAATAATCATTGGTCAACGCCTCTC	EF2276 left flank
	2196839_RS	TAGATTATCGAATATTTTCGAAATTTAATTGAATGACAAGTCGACTCAAAGTACGAGGCGATACATTGCTGATAATTTTTTAGAGTATTG	
	tetM-F	GATCAAGAAACAAAGGCAACCCAAATCTCGCAATTTGAG	*tetM* cassette
	tetM-RS	GTCAGTCGACGATCTTGTATCATTACTCCATGTATCTATTGATG	
	2196839_FB	ATGTGGATCCGAAATAAGCAATAATCATTGGTCAACGCCTCTC	EF2276 left flank-*tetM* fusion
	tetM-RS	GTCAGTCGACGATCTTGTATCATTACTCCATGTATCTATTGATG	
	2196839_FSa	TGCAGTCGACTTGTCATTCAATTAAATTTCGAAAATATTCGATAATCTA	EF2276 right flank
	2196839_RNh	GTCAGCTAGCTCAGGTGTAGAAAATTTTACTGTAGATTTTGCC	

Table S4. Plasmids used in this study.

Plasmid	Description	Reference
pKD46	Amp^R. Thermosensitive plasmid with Red lambda system	[3]
pCP20	Amp^R. Thermosensitive plasmid with FLP recombinase	[3]
pBAD18	Amp^R. Expression vector	[4]
pBT2βgal	Amp^R, GN; Cm^R, GP. Vector for allelic replacement	[5]
pRN6680	pBluescriptΩ2.9-kb pMVN6 *Sma*I-*Hind*II [*tetA(M)*]; Amp^R, Tet^R	[6]
pJP2534	pBAD18 *int-xis* P22	This work
pJP2563	pBT2βgal with *tetM* from pRN6680 positioned between *E. faecalis* V583 flanking sequences at *celA*; Cm^R, Tet^R	This work
pJP2564	pBT2βgal with *tetM* from pRN6680 positioned between *E. faecalis* V583 flanking sequences at *EF0370*; Cm^R, Tet^R	This work
pJP2565	pBT2βgal with *tetM* from pRN6680 positioned between *E. faecalis* V583 flanking sequences at *EF0394*; Cm^R, Tet^R	This work
pJP2566	pBT2βgal with *tetM* from pRN6680 positioned between *E. faecalis* V583 flanking sequences at *EF0480*; Cm^R, Tet^R	This work
pJP2568	pBT2βgal with *tetM* from pRN6680 positioned between *E. faecalis* V583 flanking sequences at *EF2276*; Cm^R, Tet^R	This work

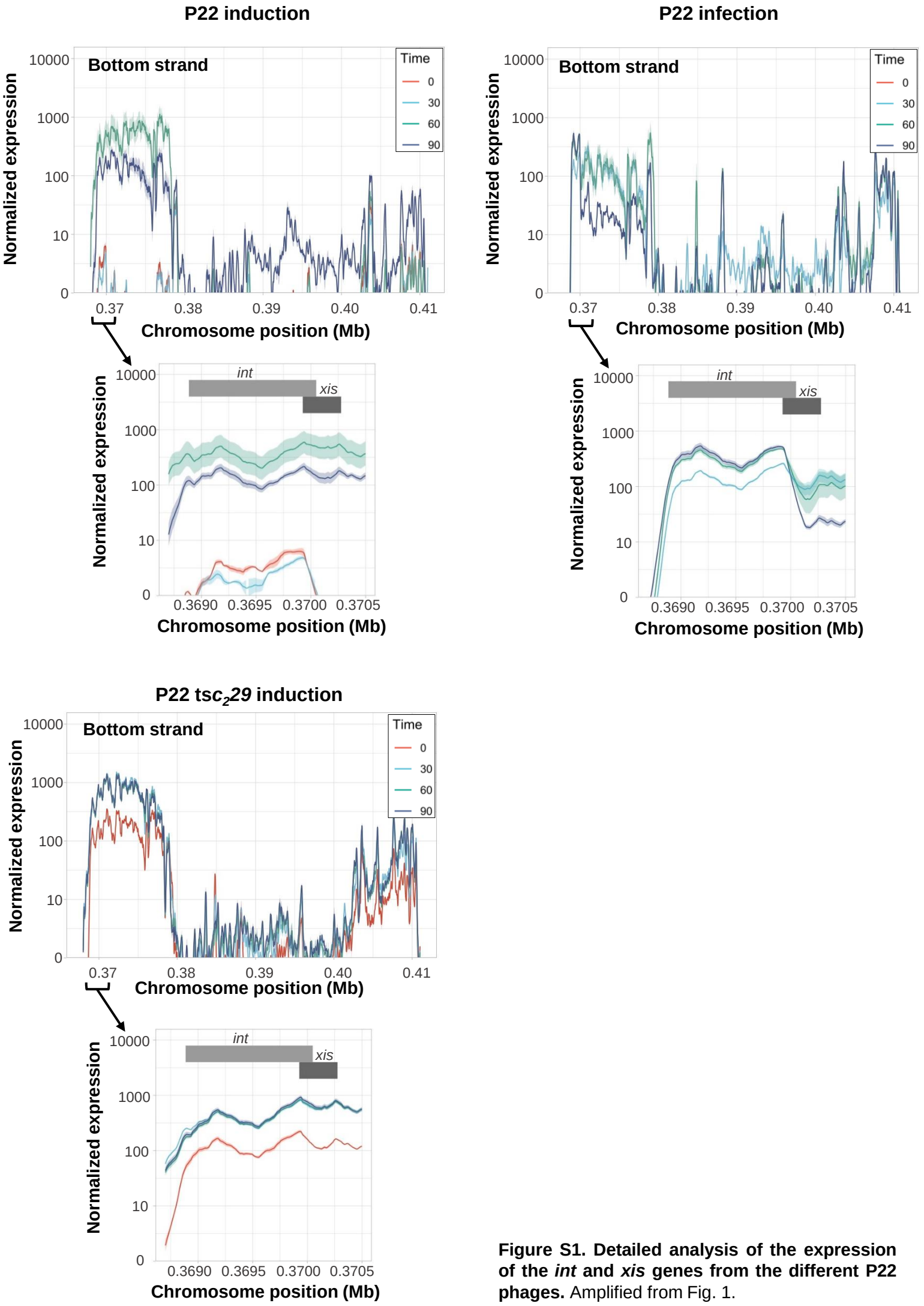
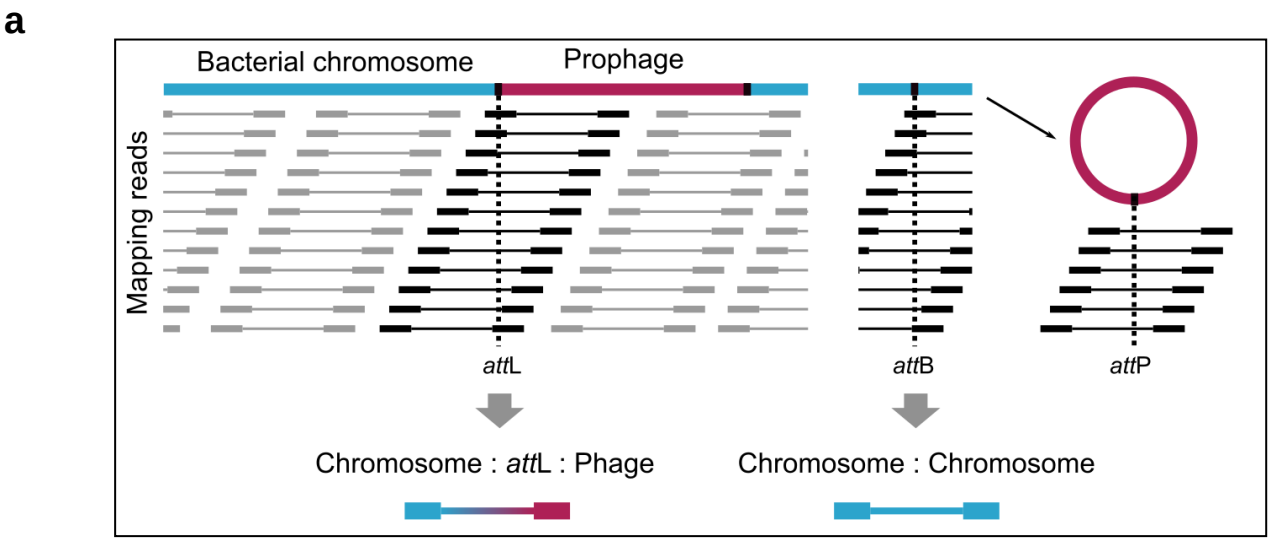
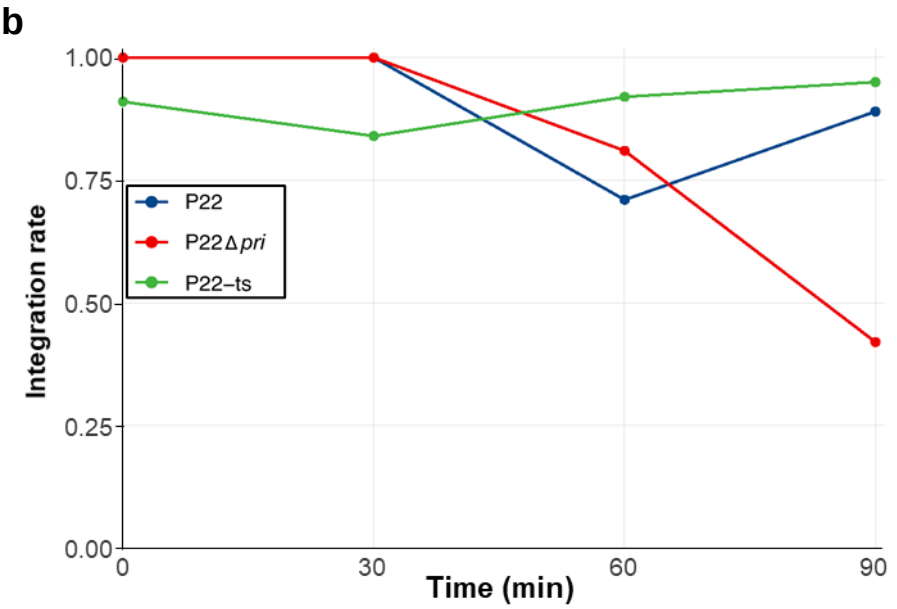


Figure S1. Detailed analysis of the expression of the *int* and *xis* genes from the different P22 phages. Amplified from Fig. 1.





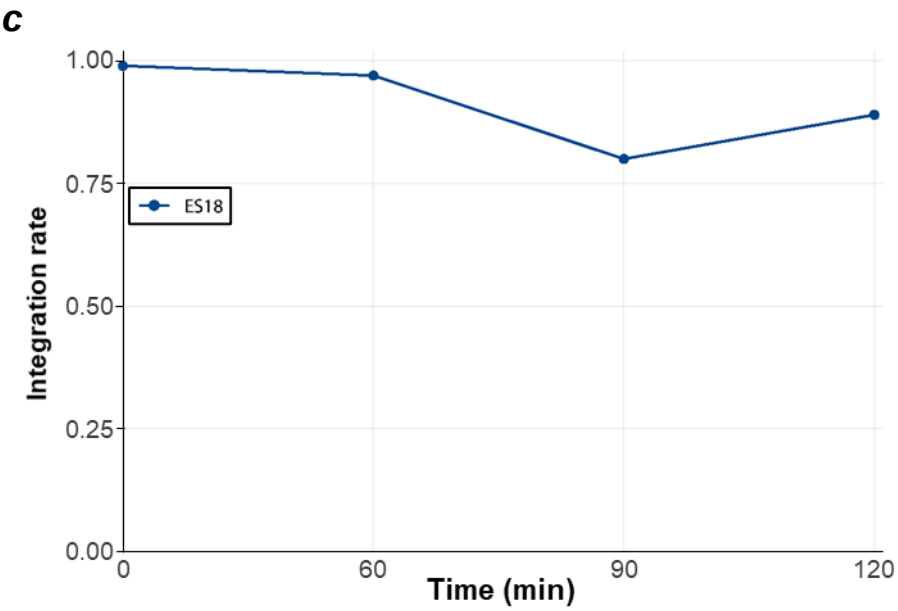


Figure S2. Prophages excise late from the bacterial chromosome.

Schematic representation of sequencing reads used for calculation of integration rate **(a)**, *att*L (left site attachment site) and *att*B (bacterial attachment site). To gain insight into the timing of phage excision, the proportion of integrated phage at each timepoint was calculated by dividing the number of chromosome-*att*L reads by the total number of *att*L/*att*B spanning reads (sum of chromosome-*att*L phage region reads plus reads spanning the *att*B region), obtained from the same sample, for phages P22, P22 Δ*pri* and P22 tsc_2*29* **(b),** and for ES18 **(c)**.

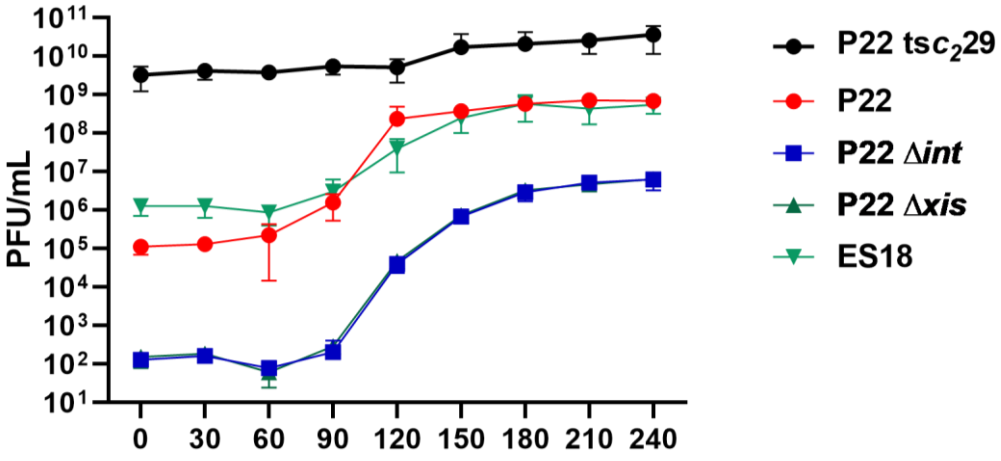


Figure S3. Phage production over a time course experiment after induction.

The lysogenic strains for phage P22, P22 Δ*int*, P22 Δ*xis,* P22 tsc_2*29* and ES18, were mitomycin C or thermal-induced to activate the prophages, samples were taken before (0) and at different time points (every 30 minutes) after induction and the phage titters evaluated (plaque forming units per milliltre: PFU/mL). The means and standard deviations from three independent experiments are presented (*n*=3).

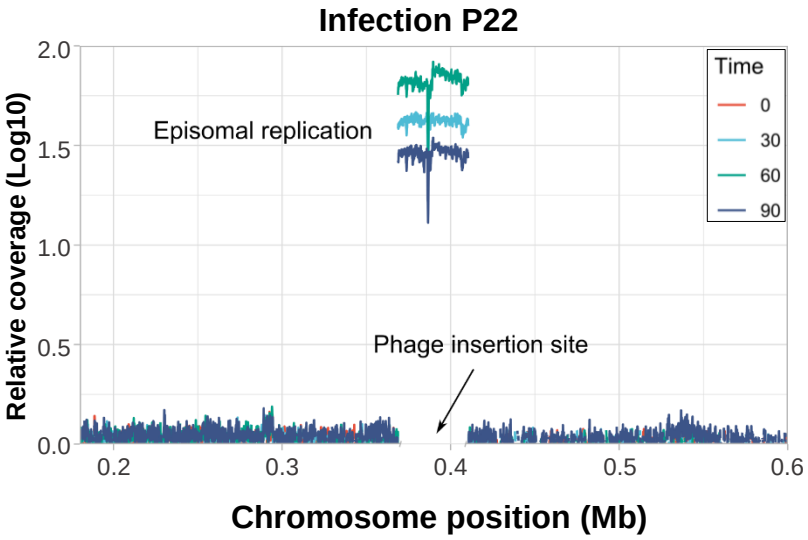


Figure S4. Phage P22 replicates extra-chromosomally after infection.

The relative abundance of phage genomic DNA and the chromosomal regions proximal to where P22 integrates is represented. Samples were analyzed at 0 (red), 30 (cyan), 60 (green), and 90 min (blue) after phage P22 infection. Relative coverage is the DNA relative to the average bacterial genomic coverage (excluding phage).

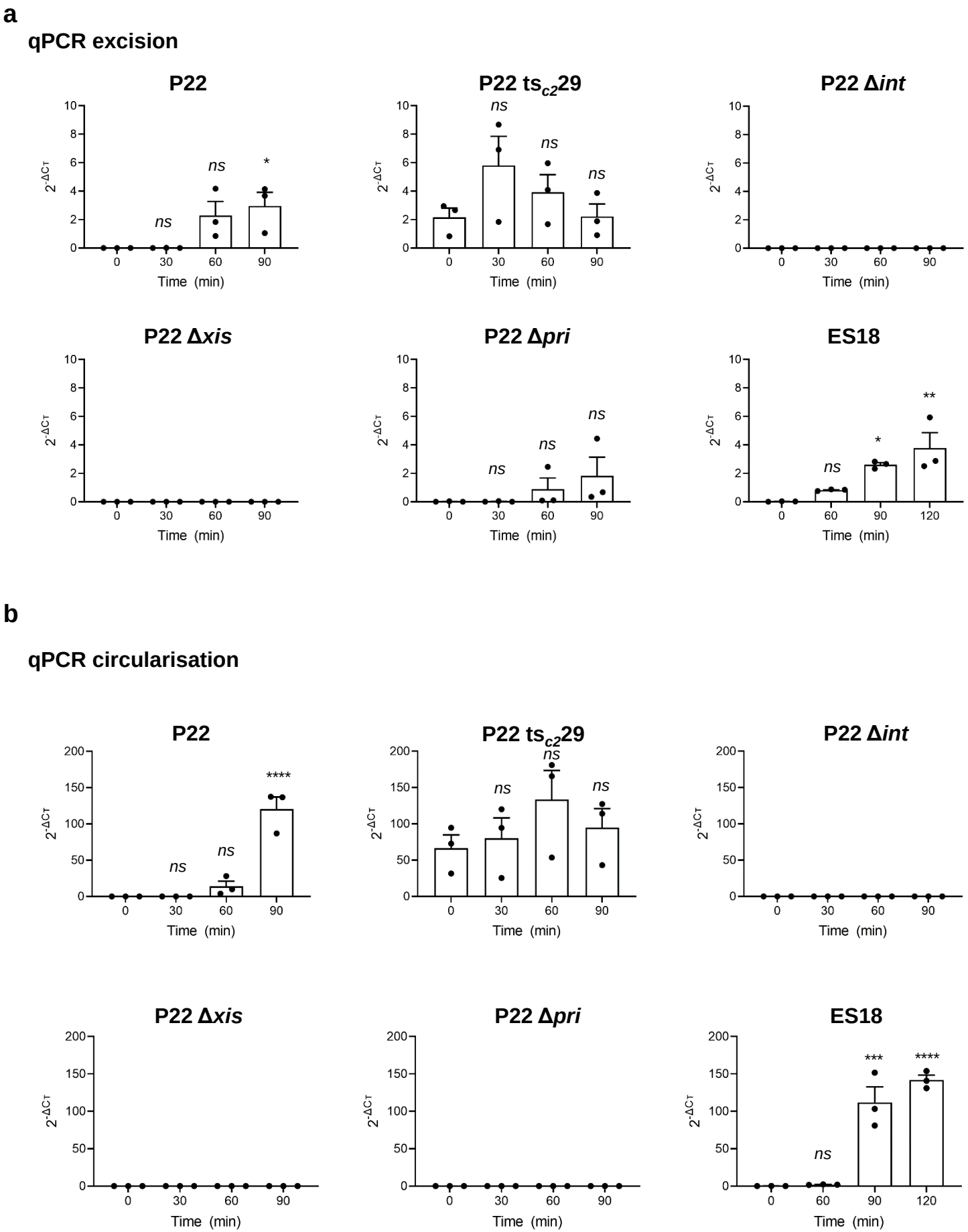


Figure S5. qPCR verification of the strains used in WGS

Analysis of the excision **(a)** or circularisation **(b)** of the different prophages after MC induction, using qPCR. Samples were analysed at 0, 30, 60, and 90 min after induction of the wt or mutants P22 prophages, or at 0, 60, 90, and 120 min after induction of the ES18 prophage (using mitomycin C or temperature-shift, as appropriate). Relative gene expression levels were analyzed by using the $2^{-\Delta CT}$ (where *CT* is threshold cycle). Error bars indicate standard deviation from the mean of three independent experiments. For all panels, values are means (n = 3 independent samples). A one-way ANOVA with Dunnett's multiple comparisons test was performed to compare time 0 against the other timepoints. Adjusted p values were as follows: *ns*>0.05; *p≤0.05; **p≤0.01; ***p≤0.001; ****p≤0.0001. The exact statistical values for each of the conditions tested are listed in Table S1.

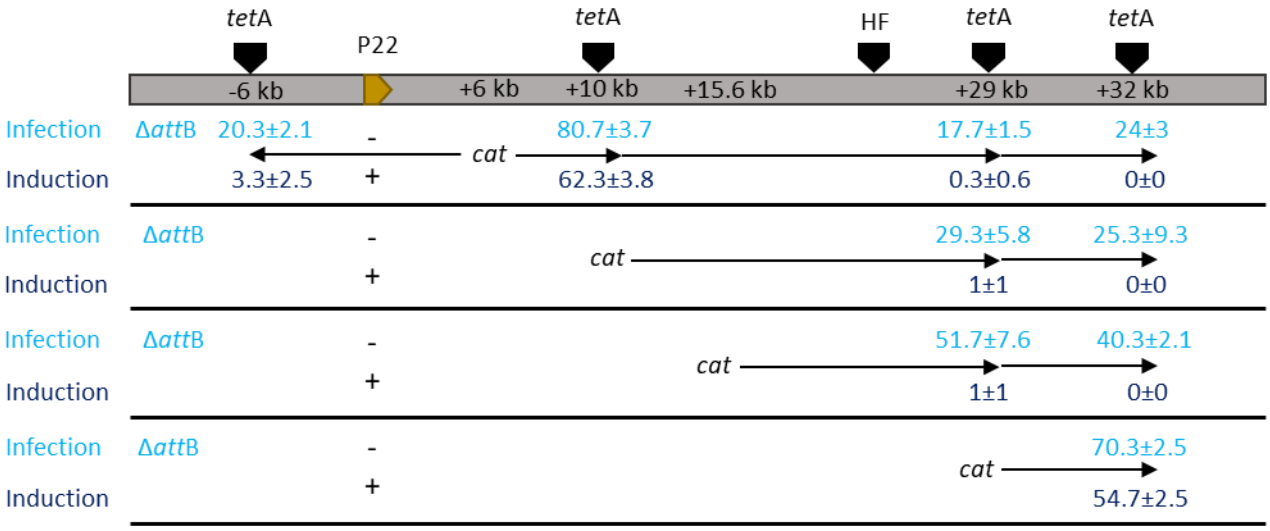


Figure S6. Lateral transduction occurs by the headful mechanism.

Co-transduction frequencies for strains containing both chloramphenicol (*cat)* and tetracycline (*tet*A) markers at varying distances apart. Lysates were tested for co-transduction of both markers by initially selecting for the *tet*A marker, with transductants subsequently scored for the *cat* marker. At least one hundred *tet*A transductants were tested from infection (cyan) or induction (blue) and the results are represented as a percentage (*cat*/*tet*A) x 100%. The *att*B for P22 is highlighted in orange and the headful limit (HF) is indicated. The + indicates a P22 lysogen (induction, LT), while the - indicates a non-lysogenic strain (infection, GT). The means and standard deviations from three independent experiments are presented (*n*=3). Our results indicate that for lysates generated by P22 infection, all co-transduction frequencies were inversely proportional to their distance apart, even if they were located in two different headfuls, indicating that DNA packaging initiated at random sites. However, when we tested lysates generated by SOS induction, co-transduction was only observed for markers within a headful, indicating that packaging had primarily initiated from the bona fide *pac* site, and confirming that P22-mediated LT uses the headful mechanism for packaging.

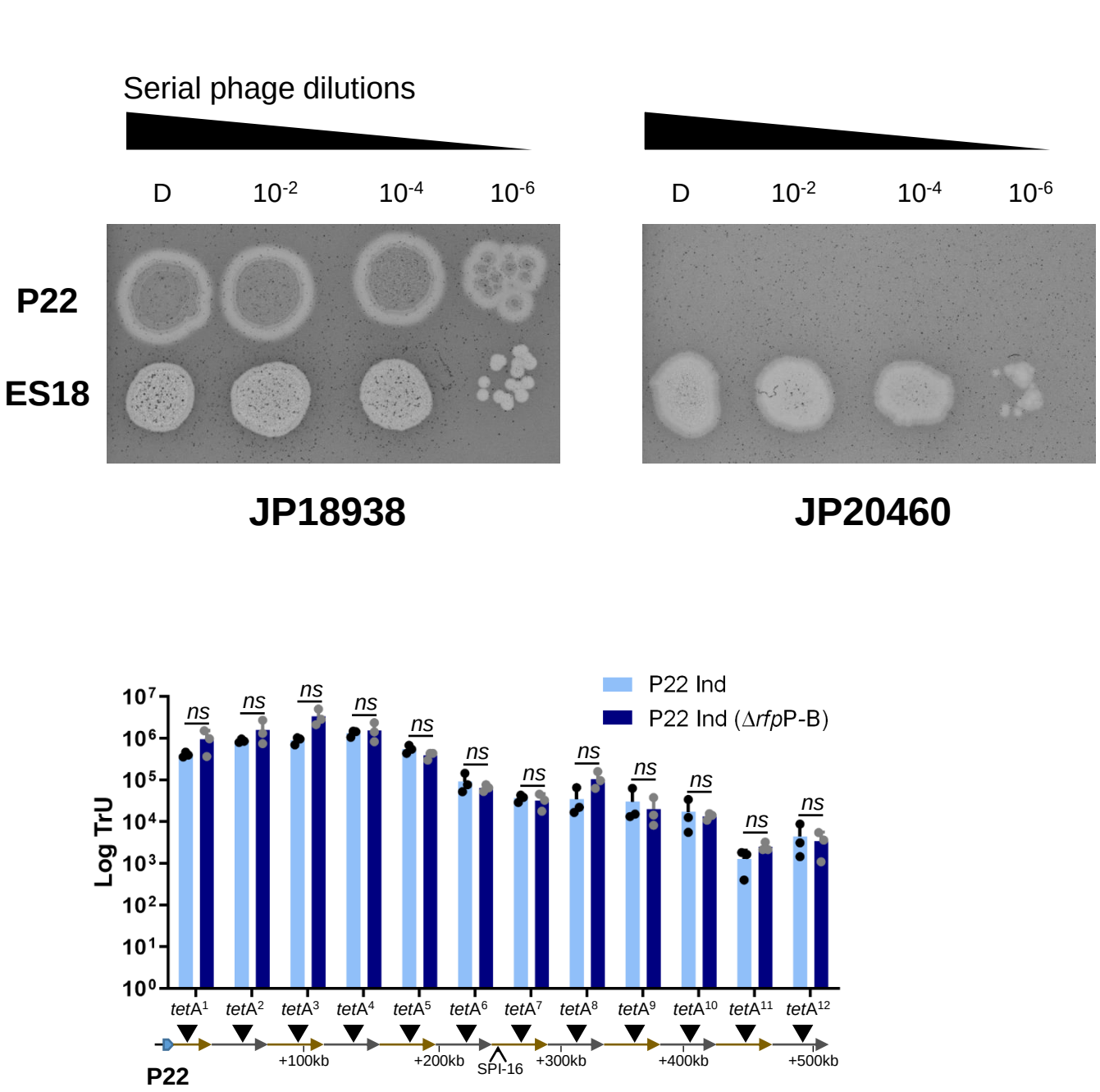


Figure S7. Phage P22 engages in lateral transduction in an infection-resistant host.

To rule out the possibility that P22 phages released early after SOS induction could superinfect the remaining cells to initiate packaging from the resident prophage genome, we deleted the *rfp*P-B genes that encode the P22 receptor and tested this strain for LT. **a,** Deletion of *rfp*PB renders LT2 insensitive to P22 infection. Serial dilutions of phages P22 and ES18 lysates were spotted onto lawns of non-lysogenic LT2 and non-lysogenic LT2 *ΔrfpP-B* strains. The presence of plaques indicates successful phage infection and replication via the lytic cycle. **b,** The transfer of tetracycline (*tet*A) markers located downstream of the P22 *att*B site, in twelve successive capsid headfuls (*tet*A$^{"n"}$), was tested after P22 induction (Ind) in either wild type LT2 or LT2 lacking the phage P22 receptor (Δ*rfp*P-B). Transduction units (TrU) per milliliter were normalized by PFU per milliliter and represented as the log TrU of an average phage titre (1 x 10^9 PFU). Error bars indicate standard deviation from the mean of three independent experiments. For all panels, values are means (n = 3 independent samples). An unpaired t test two-sided was performed to compare mean differences of infection and induction in each marker. Adjusted p values were as follows: *ns*>0.05; *p≤0.05; **p≤0.01; ***p≤0.001; ****p≤0.0001. The exact statistical values for each of the conditions tested are listed in Table S1.

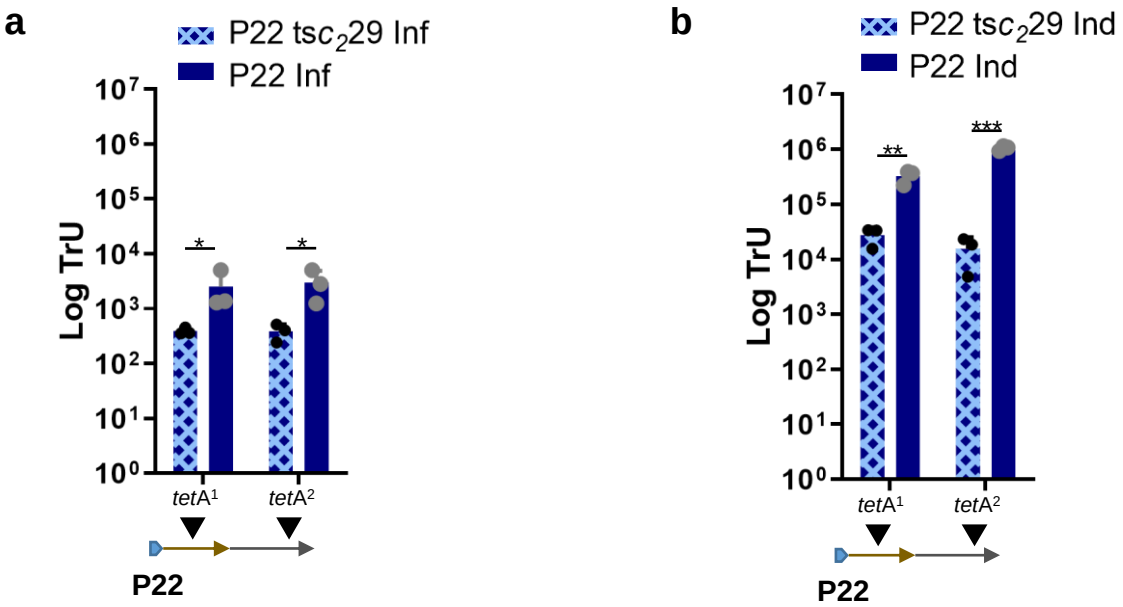


Figure S8. P22 ts$c_2$29 early excision produces low levels of lateral transduction.

a, The transfer by GT of the two first tetracycline (*tet*A) markers located downstream of the P22 *att*B site was compared for both P22 and P22 tsc_2*29* after phage infection (Inf). **b,** The transfer of the two first *tet*A markers located downstream of the P22 *att*B site was compared for both the P22 and the P22 tsc_2*29* prophages following induction (Ind). Transduction units (TrU) per milliliter were normalized by PFU per milliliter and represented as the log TrU of an average phage titre (1 x 10^9 PFU). Error bars indicate standard deviation from the mean of three independent experiments. For all panels, values are means (n = 3 independent samples). An unpaired t test two-sided was performed to compare mean differences of infection and induction in each marker. Adjusted p values were as follows: *ns*>0.05; *p≤0.05; **p≤0.01; ***p≤0.001; ****p≤0.0001. The exact statistical values for each of the conditions tested are listed on Table S1.

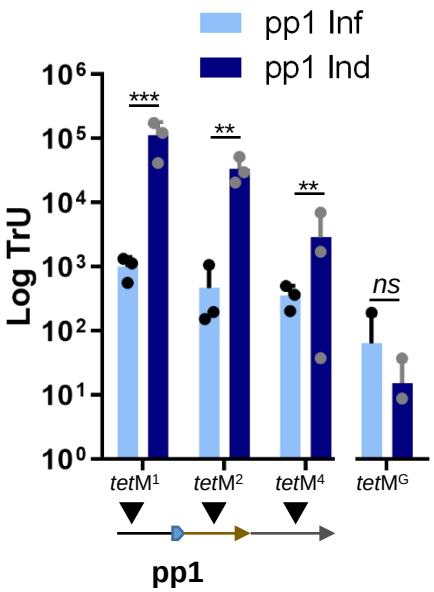


Figure S9. Enterococcal phage pp1 engages in lateral transduction.

The ability of phage pp1 to mobilise tetracycline (*tet*M) markers located downstream of the pp1 *att*B site in successive capsid headfuls (*tet*M$^{"n"}$), or from non-phage associated regions of the chromosome (*tet*M^{G}), was tested following induction (Ind) and infection (Inf). Transduction units (TrU) per milliliter were normalized by PFU per milliliter and represented as the log TrU of an average phage titre (1 x 10^9 PFU). Error bars indicate standard deviation from the mean of three independent experiments. Values are means (n = 3 independent samples). An unpaired t test two-sided was performed to compare mean differences of infection and induction in each marker. Adjusted p values were as follows: *ns*>0.05; *p≤0.05; **p≤0.01; ***p≤0.001; ****p≤0.0001. The exact statistical values for each of the conditions tested are listed in Table S1.

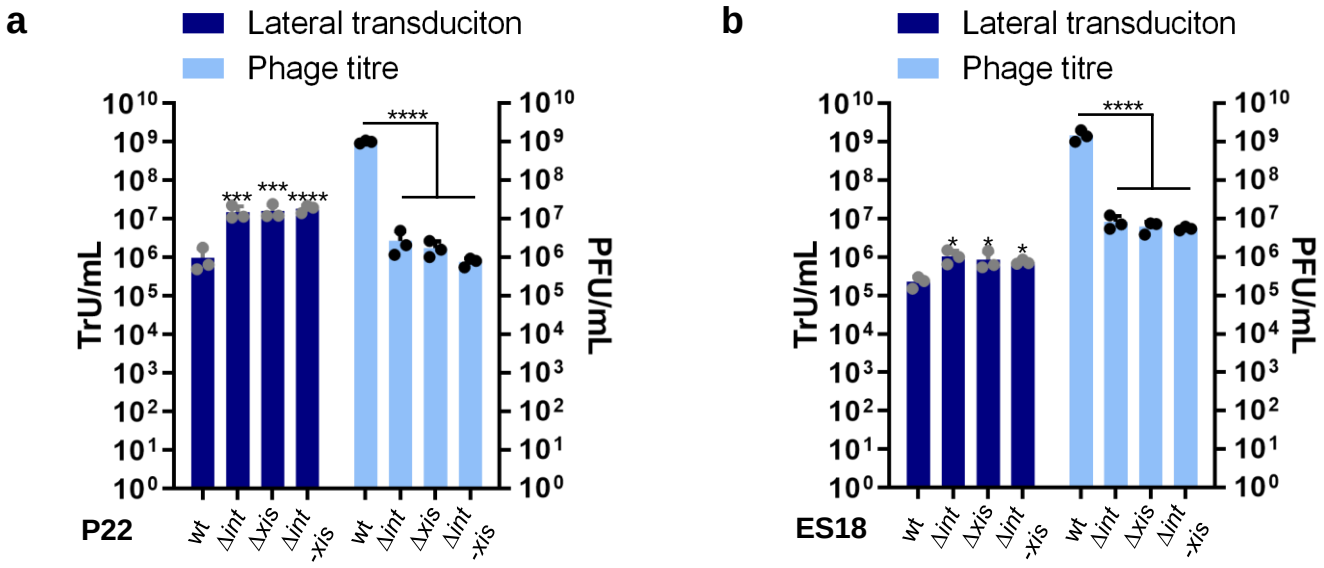


Figure S10. Effect of phage mutations on lateral transduction and phage formation.

a, P22 or P22-derivative (Δ*int*, Δ*xis* or Δ*int-xis*) prophages were mitomycin C induced and tested for their ability to transduce a *tet*A marker (TrU/ml) and produce viable phage particles (PFU/ml). **b,** The same experiment was performed using phage ES18 or ES18-derivates (Δ*int*, Δ*xis* or Δ*int-xis*). The means and standard deviations from three independent experiments are presented (*n*=3). A one-way ANOVA with Dunnett's multiple comparisons test was performed to compare mean differences between time WT and derivatives phages. Adjusted p values were as follows: *ns*>0.05; *p≤0.05; **p≤0.01; ***p≤0.001; ****p≤0.0001. The exact statistical values for each of the conditions tested are listed in Table S1.

References

1. Monk, I. R., Shah, I. M., Xu, M., Tan, M.-W. & Foster, T. J. Transforming the untransformable: application of direct transformation to manipulate genetically *Staphylococcus aureus* and *Staphylococcus epidermidis*. *MBio* **3,** (2012).
2. Matos, R. C. *et al. Enterococcus faecalis* prophage dynamics and contributions to pathogenic traits. *PLoS Genet.* **9,** e1003539 (2013).
3. Datsenko, K. A. & Wanner, B. L. One-step inactivation of chromosomal genes in *Escherichia coli* K-12 using PCR products. *Proc. Natl. Acad. Sci. U.S.A.* **97,** 6640–6645 (2000).
4. Guzman, L. M., Belin, D., Carson, M. J. & Beckwith, J. Tight regulation, modulation, and high-level expression by vectors containing the arabinose PBAD promoter. *J. Bacteriol.* **177,** 4121–4130 (1995).
5. Carpena, N., Manning, K. A., Dokland, T., Marina, A. & Penadés, J. R. Convergent evolution of pathogenicity islands in helper *cos* phage interference. *Philos. Trans. R. Soc. Lond., B, Biol. Sci.* **371,** 20150505 (2016).
6. Charpentier, E. *et al.* Novel cassette-based shuttle vector system for gram-positive bacteria. *Appl. Environ. Microbiol.* **70,** 6076–6085 (2004).